University of Crete,
Department of Biology and Medical School
Graduate Program "Molecular Biology – Biomedicine"

Institute of Molecular Biology and Biotechnology, FORTH
Gene Regulation Laboratory

Master Thesis

"Identification of genes and micro-RNAs related with the pathogenesis of Metabolic Syndrome and Type II Diabetes in mouse models"

Ioannis Evangelakos

Supervisor: Professor Kardassis Dimitris

Heraklion, August 2016

TABLE OF CONTENTS

ΠΕΡΙΛΗΨΗ

Το Μεταβολικό Σύνδρομο (ΜΣ) αποτελεί ένα σύμπλεγμα κλινικών διαταραχών όπως δυσλιπιδαιμία, διαβήτης και παχυσαρκία και σχετίζεται με αυξημένο κίνδυνο για την εμφάνιση καρδιαγγειακών νοσημάτων. Η αιτιολογία του ΜΣ είναι ελάχιστα κατανοητή ενώ αποτελεσματικές θεραπευτικές προσεγγίσεις είναι μείζονος σημασίας. Ο κύριος στόχος μας ήταν να παρακολουθήσουμε σφαιρικά τις αλλαγές στην έκφραση γονιδίων του ήπατος καθώς και των κυκλοφορούντων miRNAs που προκαλούνται κατά την παθογέννεση του ΜΣ στο διαγονιδιακό στέλεχος ποντικού APOE3L.CETP που χρησιμοποιήθηκε ως μοντέλο του ΜΣ. Αρσενικά ποντίκια έλαβαν είτε υψηλή σε λιπαρά (HFD) είτε χαμηλή σε λιπαρά (LFD) δίαιτα για συγκεκριμένες χρονικές περιόδους. Το μεταγραφικό προφίλ του ήπατος αναλύθηκε σε μικροσυστοιχίες της Affymetrix ενώ η αλλαγμένη έκφραση συγκεκριμένων γονιδίων πιστοποιήθηκε και με RT-qPCR ανάλυση και ακολούθησε εκτενής βιοπληροφορική ανάλυση. Ολικά miRNAs απομονώθηκαν από τον ορό του αίματος και τα επίπεδά τους ποσοτικοποιήθηκαν με RT-qPCR. Τα αποτελέσματα έδειξαν πως η διατροφική παρέμβαση είχε ισχυρές επιπτώσεις στην έκφραση διαφόρων γονιδίων του ήπατος. Επιπλέον, στον ορό των APOE3L.CETP ποντικών ανιχνεύτηκαν miRNAs που είχαν προηγουμένως συσχετιστεί με μεταβολικές διαταραχές και συγκεκριμένα τα επίπεδά τους ήταν αυξημένα ως απόκριση στην υψηλή σε λιπαρά δίαιτα για 12 εβδομάδες. Από τα δεδομένα των μικροσυστοιχιών προσπαθήσαμε να ανιχνεύσουμε νέα γονίδια του ήπατος με αλλαγμένη έκφραση που να είναι πιθανοί στόχοι των συγκεκριμένων miRNAs. Εξόρυξη δεδομένων και βιοπληροφορική ανάλυση των αποτελεσμάτων από το μεταγραφικό αποτύπωμα του ήπατος ανέδειξε πως τα επίπεδα έκφρασης της κινάσης Sik1 (Salt Inducible kinase 1) ήταν μειωμένα στο ήπαρ των APOE3L.CETP ποντικών που είχαν λάβει υψηλή σε λιπαρά δίαιτα για 12 εβδομάδες. Επιπλέον, η κινάση Sik1 αποτελεί πιθανό στόχο του miR-27a το οποίο βρέθηκε αυξημένο στην κυκλοφορία των ίδιων ποντικών. Έτσι, υποθέσαμε την ύπαρξη μιας εύλογης αλληλεπίδρασης μεταξύ των δύο μορίων και προσπαθήσαμε να ανιχνεύσουμε ένα πιθανό μηχανισμό ρύθμισης. Ακόμη, χρησιμοποιήσαμε το διαβητικό μοντέλο ποντικού $Akt2^{-/-}$ προκειμένου να μελετήσουμε αν τα αλλαγμένα επίπεδα των κυκλοφορούντων miRNAs οφείλονται σε διαβητικές παραμέτρους. Συμπερασματικά, τα αποτελέσματά μας αναδεικνύουν χαρακτηριστικές αλλαγές στην

έκφραση γονιδίων του ήπατος αλλά και στα επίπεδα συγκεκριμένων miRNAs τόσο στο Μεταβολικό Σύνδρομο όσο και στον Διαβήτη τύπου ΙΙ, τα οποία θα μπορούσαν να αξιοποιηθούν περεταίρω για διαγνωστικές ή θεραπευτικές προσεγγίσεις.

ABSTRACT

The metabolic syndrome (MetS) is a cluster of clinical disorders such as dyslipidemia, diabetes and obesity which are associated with increased risk for cardiovascular disease. The etiology of MetS is poorly understood and effective therapies are urgently needed. Our main goal was to monitor global changes in the expression of hepatic genes and circulating miRNAs during the pathogenesis of the MetS in the transgenic strain APOE3L.CETP mice that was used as a model of MetS. Male mice were fed either a High (HFD) or a Low (LFD) Fat Diet for different time periods. Liver RNA was analyzed on Affymetrix Mouse Gene 2.0 ST arrays and data were validated by RT-qPCR followed by bioinformatical analysis. Total miRNAs were isolated from serum and quantitated by RT-qPCR. We found that the dietary intervention had a strong impact on the expression of hepatic genes in APOE3L.CETP mice. In addition, miRNAs previously correlated to metabolic disorders were detected in the serum of APOE3L.CETP mice and their levels were increased in response to a 12 week HFD administration. From our microarray data we tried to identify novel differentially expressed hepatic genes that seem to be predicted targets of our miRNAs. Data mining in the transcriptomic analysis revealed that Sik1 (Salt Inducible kinase 1) was deregulated in livers of 12 week HFD-diet APOE3L.CETP mice and simultaneously was predicted as a target of miR-27a which was found elevated in the plasma. We therefore hypothesized a plausible interaction between these two molecules and tried to identify a potential regulatory mechanism. Moreover, we used the diabetic Akt2$^{-/-}$ mouse model to test whether the differential detection of the circulating miRNAs was attributed to diabetic parameters. In conclusion, our findings reveal for the first time characteristic hepatic gene and plasma miRNA signatures during the pathogenesis of MetS and Type II diabetes which could be exploited further for diagnostic or therapeutic purposes.

INTRODUCTION

i) Metabolic Syndrome

Metabolic Syndrome (MetS) is a complex disorder and one of the major health challenges of this century, mainly due to major changes in life habits, the surplus daily energy intake and the increasing rate of obesity. MetS refers to a combination of several physiological, biochemical, clinical and metabolic disorders that could potentially raise the risk for atherosclerotic cardiovascular diseases, obesity and type II diabetes (Alberti et al., 2005; Kaur, 2014; van den Hoek et al., 2014). Some features that characterize MetS are increased visceral adiposity, elevated blood pressure, hypertriglyceridemia, low levels of high-density lipoprotein (HDL) cholesterol accompanied by high levels of low-density lipoprotein (LDL) cholesterol and impaired glucose tolerance or insulin resistance (Figure1) (Ford et al., 2002; Reilly and Rader, 2003). It is generally accepted that a patient is characterized as MetS when at least three of the above clinical features are present (Alberti et al., 2009).

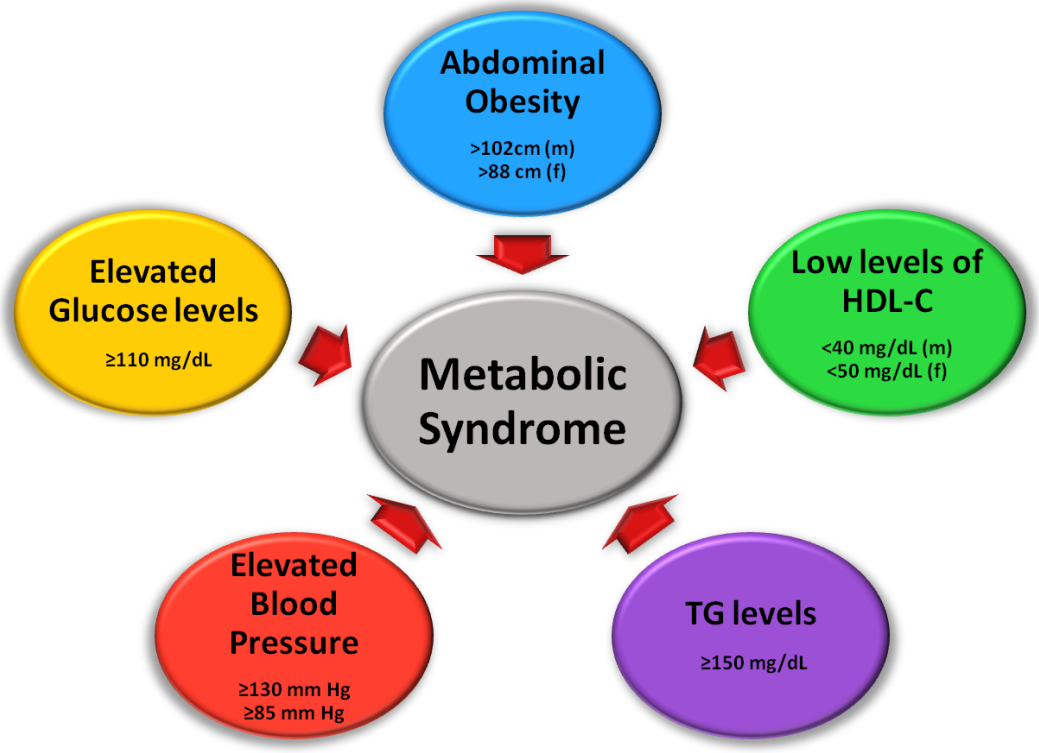

Figure 1: The five clinical features of the metabolic syndrome.

The pathogenesis of the Metabolic Syndrome is not yet fully characterized. However, it seems that the initiation of the syndrome is attributed to a combination of genetic predisposition of polygenic origin with a sedentary lifestyle and an excess calorie diet. Furthermore, nutrient excess leads to rapid alterations in adipose tissue physiology such as enlargement of adipocytes, enhanced macrophage infiltration and overproduction of adipocytokines and proinflammatory molecules including TNF-a, IL-1β and IL-6 (Hajer et al., 2008). These molecules can promote lipid accumulation and exert deleterious effects on blood vessels, mainly by promoting endothelial dysfunctions thus increasing the risk for myocardial infraction, stroke and cardiomyopathies (Leon and Maddox, 2015). As a result, MetS is accompanied by a systemic low-grade inflammatory state which is attributed to the interaction between environmental and genetic factors (Moller and Kaufman, 2005) and in combination with the general dyslipidemia it has been shown to increase the risk for cardiovascular diseases and atherosclerosis (Genser et al., 2016; Vassallo et al., 2016).

The Metabolic Syndrome has been also associated with atherosclerosis development. Atherosclerosis is mainly attributed to the initial accumulation of lipoprotein particles in the intima of the arterial walls (Lusis, 2000). This process leads to the recruitment of monocytes at these sites and their transmigration into the intima. Afterwards, monocytes differentiate into macrophages and begin to take up cholesterol. When the macrophages are cholesterol-loaded (called “foam cells”) they die and their lipid content is released to the necrotic areas, a process that eventually leads to necrotic plaques that are generally observed in patients that develop atherosclerosis (Ross, 1993).

HDL is the main particle with atheroprotective effects as it mediates the efflux of excess cholesterol from a variety of tissues (Kardassis et al., 2014; Vaziri, 2016). Raising HDL cholesterol levels has been proposed as a promising strategy for alleviating dyslipidemia and atherosclerosis. However, recent studies have shown that the HDL-rising therapeutic approaches have controversial effects in patients with cardiovascular diseases (Kakafika et al., 2008; Tariq et al., 2014). So now researchers shift their attention on how HDL can effectively remove cholesterol from macrophage foam cells and transfer them to the liver, a process that has been termed “Reverse Cholesterol

Transport" (RCT). Independently of its quantity in the circulation, it seems that HDL's function must be effective in order to exert its protective roles in cardiovascular and metabolic diseases.

Liver is the responsible organ for HDL's biogenesis where ABCA1 transporter mediates the lipidation of lipid-poor ApoA-I (the main protein component of HDL) to form the nascent HDL which can acquire phospholipids (PL) and free cholesterol (FC) from both liver and peripheral tissues. Lecithin-cholesterol acyl transferase (LCAT) catalyzes the conversion of nascent HDL to mature HDL with a parallel esterification of FC to cholesterol esters (CE) (Besler et al., 2012; Kardassis et al., 2014). Cholesteryl Ester Transfer Protein (CETP) is the responsible enzyme for the transfer of CE from HDL to VLDL and LDL in exchange for triglycerides. Interestingly, transgenic mice expressing CETP (which normally don't) present a shifted distribution of cholesterol between lipoproteins, depicted in increased cholesterol in VLDL/LDL and reduced in HDL particles. (Westerterp et al., 2006). The Scavenger Receptor class B type I (SR-BI) is a crucial receptor in cholesterol metabolism as it facilitates the uptake of FC and CE from HDL thus promoting the excretion of excess cholesterol from the liver to the bile (through specific receptors such as ABCG5/8). SR-BI is also present in the adrenals where it facilitates the uptake of CE from HDL to be used as a precursor for the synthesis of steroid hormones (Out et al., 2004).

In addition, one of the most prominent phenotypic effects of the Metabolic Syndrome is the accumulation of lipids in the liver (the so called fatty liver) which promotes liver steatosis and Non Alcoholic Fatty Liver Disease (NAFLD). Interestingly, lipid deposition in liver has already been characterized as the hepatic manifestation of the syndrome (Lonardo, 1999; Marchesini et al., 2001). Patients and rodents with fatty liver disease present active adipogenesis in the liver, which is depicted in the increased expression of master regulators of adipogenesis such as Peroxisome Proliferator-Activated Receptor γ (PPARγ) and Sterol Regulatory Element Binding Protein 1c (SREBP-1c).

The growing incidence of Metabolic Syndrome has become a worldwide clinical and public threat by increasing morbidity and mortality. Despite the fact that bariatric surgery has had an enormous impact on the treatment of metabolic syndrome,

improved and novel therapeutic strategies must be established. Since the main cause of the metabolic syndrome remains unknown, researchers are reverting back to the elucidation of the molecular mechanisms that underlie MetS in order to gain insight on the exact pathogenic factors and design effective pharmacological approaches.

For all the above reasons and since the liver is the crucial organ that controls lipid and glucose homeostasis, it is anticipated that the identification of gene expression changes in Metabolic Syndrome could shed light into the molecular mechanisms being involved in the pathogenesis of the disease.

ii) Type II Diabetes

Diabetes mellitus in its simplest definition is considered to be a chronic metabolic disorder characterized by high blood glucose levels. The main forms of diabetes mellitus are Type I, resulting from decreased insulin production from the pancreas and Type II, characterized by impaired response of peripheral tissues to insulin (insulin resistance).

Insulin is secreted from β-pancreatic cells and facilitates blood glucose uptake by various cells, including skeletal muscle cells and adipocytes. Furthermore, insulin is responsible for the conversion of excess glucose to glycogen for further storage in organs such as the liver and the muscles.

Type II Diabetes mellitus (T2DM) is a complex heterogeneous group of metabolic dysfunctions including hyperglycemia, insulin resistance and failure of pancreatic β-cells to secrete insulin in response to elevated blood glucose (Lin and Sun, 2010). Three crucial defects have been associated with the onset of hyperglycaemia in T2DM: a) increased hepatic glucose production, b) decreased insulin secretion and c) disturbed insulin action (Stumvoll et al., 2005). The pathogenesis of T2DM is polygenic in origin, with genetic predisposition and physical inactivity to exert pivotal roles, but yet its etiology has not been fully elucidated. It was reported that in 2011, 366 million people suffered from T2DM and it is estimated that by 2030 the number of patients will have been rocketed to 552 millions. The worldwide prevalence of T2DM in adults is predicted

to be even more prominent in the future mainly due the new lifestyle, rendering this disease as one of the most severe clinical challenges.

Obesity has already been associated with T2DM as it represents a high risk factor for the development of the disease. Visceral obesity promotes fat storage in adipose tissue and other organs such as liver and muscles (Guilherme et al., 2008). At the same time, the high levels of free fatty acids in the circulation disrupt the insulin signaling pathways resulting in insulin resistance, which constitutes one of the crucial events in the development of T2DM and Metabolic Syndrome (DeFronzo, 1992; Rask-Madsen and Kahn, 2012; Yki-Jarvinen, 1995).

At the molecular level and under normal conditions, when blood glucose levels are increased insulin is produced by the pancreas and is secreted to the circulation. Insulin acts through the insulin receptor (IR) which becomes tyrosine-phosphorylated and in turn activates the downstream signaling cascade of IRS-1/PI3K/Akt. This signaling pathway leads to the translocation of GLUT4, the main glucose transporter, to the cell membrane, facilitating glucose uptake from the bloodstream (Figure 2).

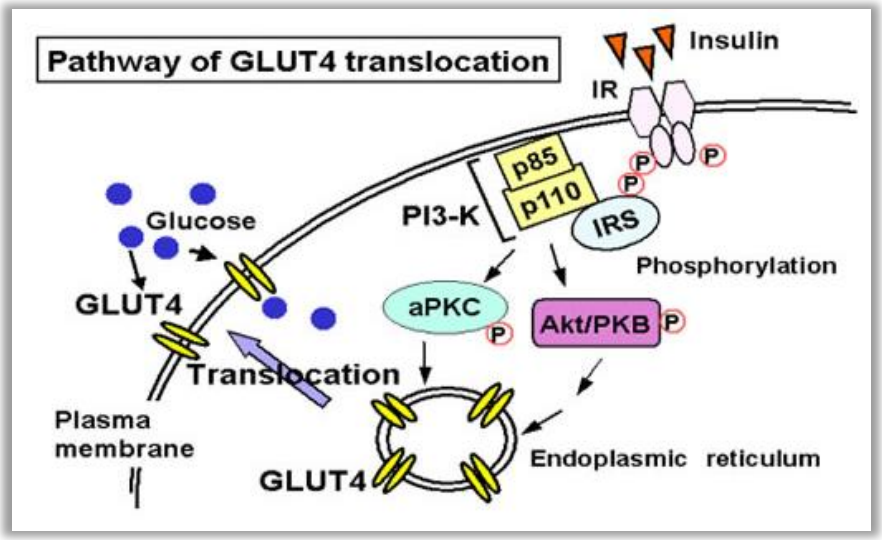

Figure 2: Insulin action in activating GLUT4 translocation to the cell membrane.

Under insulin resistance conditions, several tissues are affected (including liver and skeletal muscles) and cannot respond effectively to insulin signals. As a result, the

above pathway is impaired and glucose remains in the circulation leading to hyperglycaemia (Figure 3) (DeFronzo and Tripathy, 2009; Rask-Madsen and Kahn, 2012).

Current theories on the pathogenesis of T2DM underline several defects in the organs of the body. Initially, adipose tissue seems to exert an increased secretion of free fatty acids accompanied with low secretion of regulatory factors such as adiponectin. Skeletal muscle cells, which facilitate almost the 75% of the whole body insulin-stimulated glucose uptake, present decreased insulin/PI3K/Akt signaling and are becoming insulin resistant. Central nervous system seems to have impaired sensing and response to hyperglyceamia while liver presents a prominent dysregulated insulin action which leads to hepatic glucose production (Lin and Sun, 2010).

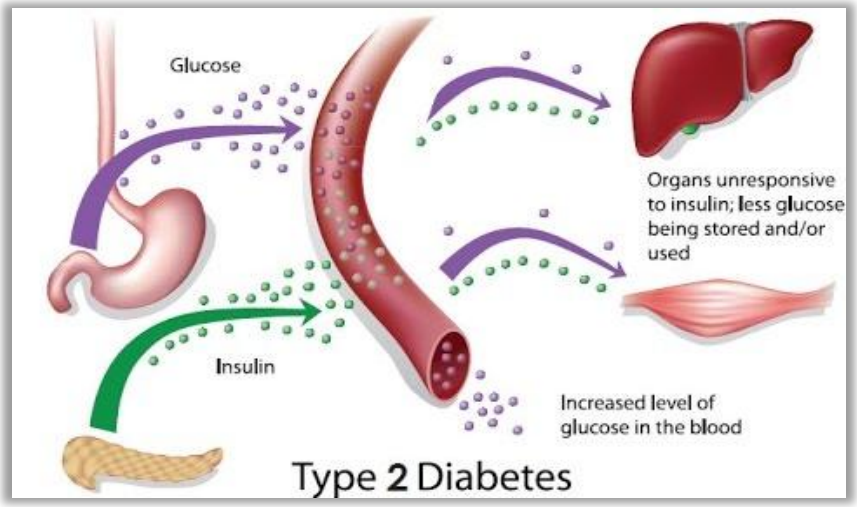

Figure 3: Insulin action is disturbed in T2DM, leading to excess glucose in the blood.

It has been reported that in insulin resistant skeletal muscles of rodents fed with a high-fat diet there is an increased fatty acid flux from the circulation accompanied with a transient increase of the intracellular levels of diacyloglycerol (DAG) (Figure 4). The lipid intermediate DAG can activate several isoforms of the protein kinase C (PKC) family which mediate the serine phosphorylation of IRS-1 (insulin receptor substrate 1). This phosphorylation inhibits the tyrosine phosphorylation of the substrate which is necessary for the downstream binding to PI3K (Samuel et al., 2010; Shulman, 2014a). This eventually leads to a decreased insulin-stimulated glucose transport activity.

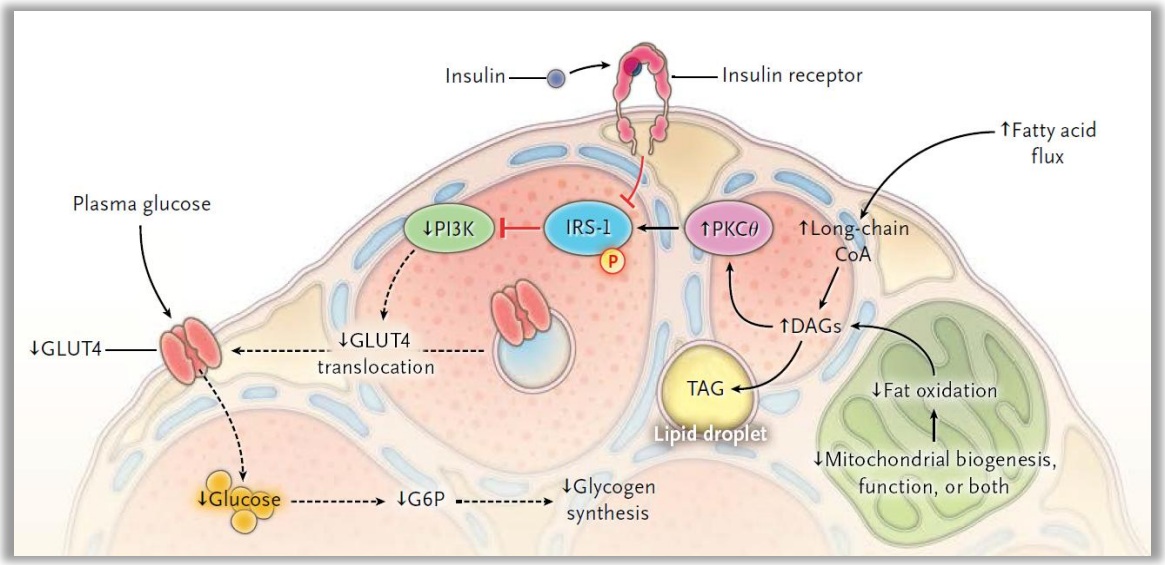

Figure 4: Lipid induced insulin resistance in muscles (Shulman, 2014b).

Furthermore, insulin resistance affects the physiology of the liver in T2DM. DAG accumulation in the liver activates an isoform of PKC which in turn phosphorylates and inactivates the IR, inhibiting the activation of PI3K and Akt2 which normally promote glycogen synthesis and decrease gluconeogenesis (Figure 5). As a result, FOXO1 and FOXA2 transcription factors are activated and translocate to the nucleus where they mediate the transcription of gluconeogenic genes. Consequently, liver becomes insulin resistant, glucose production is triggered while its uptake in diminished.

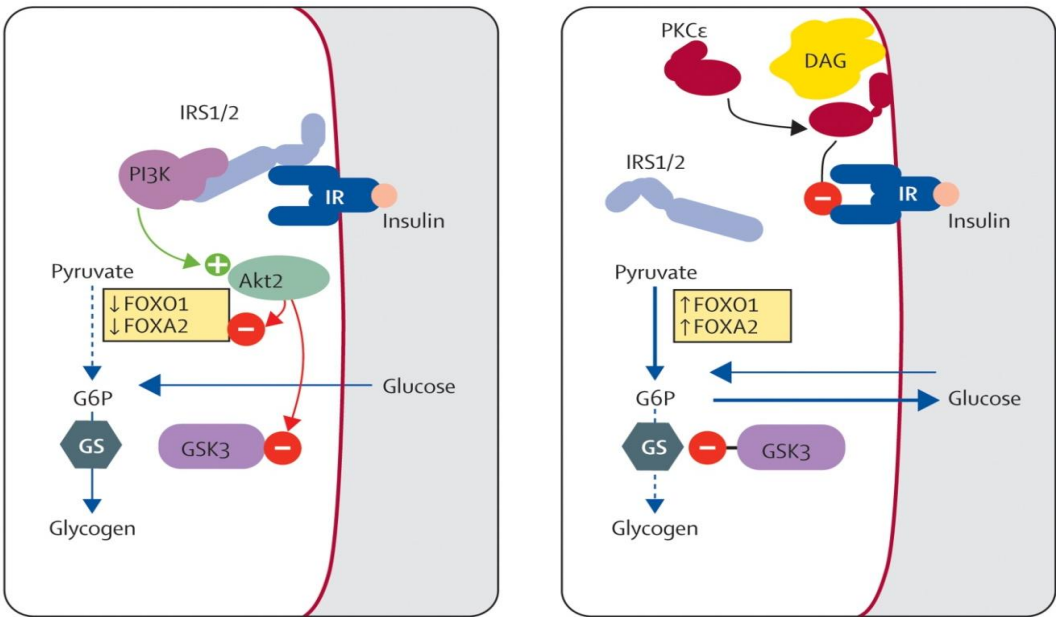

Figure 5: Lipid induced insulin resistance in liver (Samuel et al., 2010).

iii) microRNAs

MicroRNAs (miRNAs or miRs) constitute an evolutionarily conserved class of non-coding RNAs of 18-25 nucleotides that are encoded initially as long primary transcripts (pri-miRNAs) by the genome (Figure 6). The molecular machinery of the cells (RNase III enzymes Drosha and Dicer) cleaves the pri-microRNAs to produce the pre-microRNAs (~70 nucleotides) and consequently the mature microRNAs. Dicer generates imperfect dublexes of ~22 nucleotides consisting of a guide strand ("miRNA" or "predominant product" as referred in miRBase) and a passenger strand ("miRNA*" or "the opposite arm of the precursor" as referred in miRBase). Furthermore, especially when data are not sufficient to determine the predominant product, miRNAs are usually symbolized as "miR-X-5p" or "miR-X-3p", relative to the arm from which they are produced. In association with RISC complex (RNA Induced Silencing Complex), the guide strand-miRNAs exert important functions in gene regulation, mainly by acting as negative regulators of gene expression. On the other hand, the passenger strands are usually degraded but sometimes may be also functional. Since their first discovery in *C. elegans* (Lee et al., 1993; Wightman et al., 1993) more than 800 members have been identified in humans and it is proposed that almost the one-third of all genes are predicted to be under control of microRNAs.

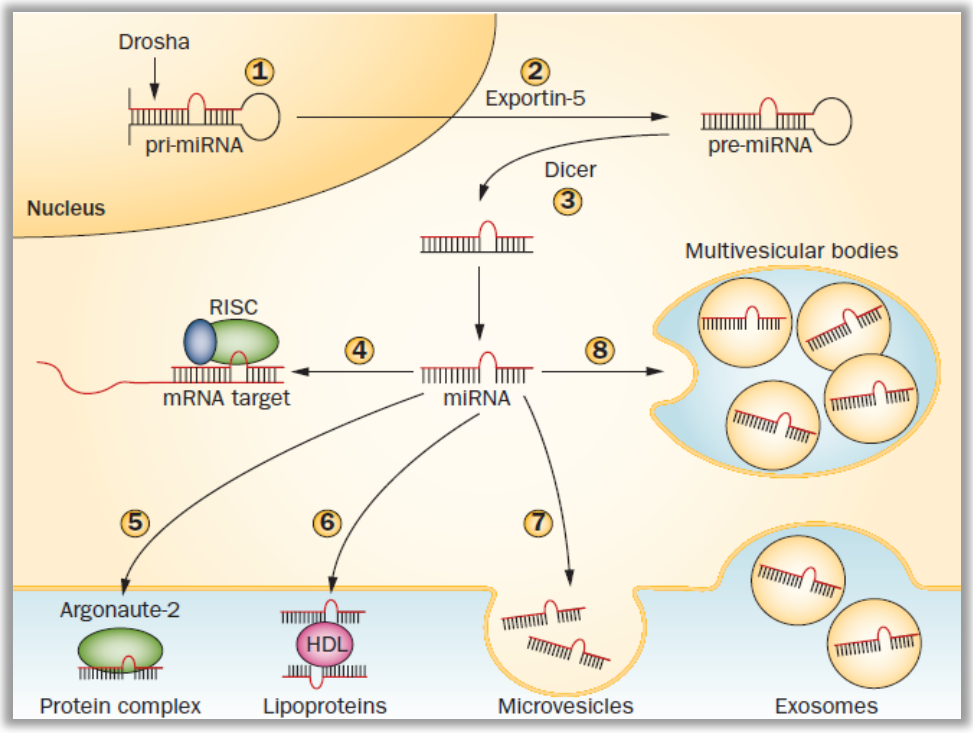

Figure 6. Biogenesis of miRNAs from pri-miRNAs and several pathways that they follow. Drosha cleaves pri-miRNA producing the pre-miRNA in the nucleus (1), exportin-5 is the responsible enzyme for pri-miRNA export to the cytoplasm (2) where finally Dicer cleaves the pre-miRNA producing the mature miRNA (3). The miRNAs then can associate with RISC complex and target mRNAs for degradation (4), bind to RNA-binding proteins such as Argonaute-2 protein complex (5) or to lipoproteins (6). Furthermore, miRNAs can be loaded in microvesicles (7) or in exosomes (8) and then be released extracellularly (Guay and Regazzi, 2013).

Two well established mechanisms exist about gene regulation through microRNAs a) the translational repression of protein coding genes and b) microRNA-mediated mRNA cleavage and degradation (by partially pairing to the 3' untranslated region of the target mRNA, 3'UTR) (Jackson and Standart, 2007). It is widely known that microRNAs control fundamental intracellular metabolic pathways related with fat metabolism, energy homeostasis, differentiation of adipocytes, insulin secretion and inflammation (Esau et al., 2006; Poy et al., 2004). MicroRNAs have recently emerged as crucial post-transcriptional regulators of several metabolic disorders, underlying their importance both as potential biomarkers that could warn prior to the disease development or as novel class of targets for therapeutic manipulation.

Except from their intracellular localization, miRNAs can also be found in blood and other body fluids in association with proteins, microvesicles, exosomes or lipoprotein complexes the so called "circulating miRNAs" (Arroyo et al., 2011; Vickers et al., 2011). These miRNAs have already gathered a lot of attention by the scientific community and research concerning their regulatory roles has become increasingly frequent. Once produced in one cell type they can be secreted in peripheral blood and exert their regulatory role in distal cells or tissues (Figure 7). In several studies it has been shown that circulating miRNAs play significant roles in maintaining metabolic homeostasis and thus they could possibly serve as potential therapeutic targets in metabolic disorders such as MetS (Heneghan et al., 2011; Zampetaki et al., 2010).

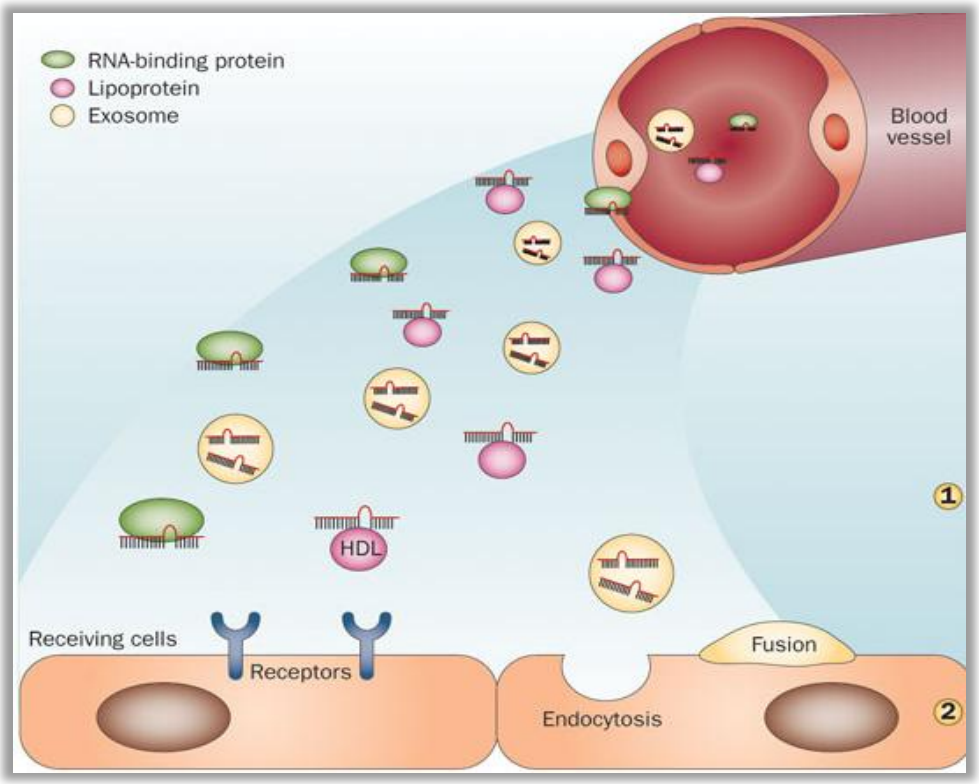

Figure 7. Circulating miRNAs in blood and body fluids. miRNAs can be taken up from the blood through specific receptors (1) or by endocytosis of the relative exosome (2) (Guay and Regazzi, 2013).

During this project we wanted to monitor the expression levels of specific circulating miRNAs in metabolic disorders in order to unravel their potential roles in the regulation of several metabolic genes. Furthermore, these miRNAs could be used as biomarkers for these diseases or potential targets for therapeutic approaches.

To be more specific, we decided to analyze 9 particular miRNAs that were previously correlated with metabolic diseases in animal models of MetS and Type II Diabetes. These 9 miRNAs are: miR-27a, miR-130b, miR-135a, miR-223, miR-375, let-7b, miR-192, miR-194 and miR-193b (Table 1).

Table 1: The 9 analyzed miRNAs, their validated targets and several roles or experimental observations related to metabolic diseases

miRNA	Targets	Several Roles / Experimental Observations
miR-27a	**FOXO1** **PPARγ** **SREBP1-2** **RXRα** **HOXA5/HOXA10**	• Regulates fat synthesis by supressesing lipid synthetic genes such as *SREBP1-2* and *FASN* *(Shirasaki et al., 2013)* • Negative regulator of adipocyte differentiation *(Lin et al., 2013)* • Over-expression → suppresses PPARγ levels *(Kim et al., 2010)* • Upregulated in the circulation in MetS patients *(Karolina et al., 2012)* • Increased in the circulation in T2DM *(Villard et al., 2015)*
miR-130b	**PPARγ** **PGC1-a** **ABCA1**	• Correlated with obesity, upregulated in the circulation of obese mice *(Wang et al., 2013b)* • Over-expression → reduces adipogenesis *(Chen et al., 2015)* • Risk factor for Metabolic Syndrome *(Wang et al., 2013b)*
miR-135a	**FOXO1** **IRS2** **APC**	• Suppresses adipogenesis through activation of Wnt pathway *(Chen et al., 2014)* • Inhibits insulin signaling and glucose uptake by targeting IRS2 *(Agarwal et al., 2013)* • miR silencing → alleviates hyperglycemia, improves glucose tolerance *(Agarwal et al., 2013)*
miR-223	**FOXO1/3** **MEF2C/2D** **IGFR** **HMGCS1** **SR-BI**	• Incorporation and transport by HDL particles *(Rottiers and Naar, 2012; Vickers et al., 2011)* • Regulates GLUT4 expression and cardiomyocyte glucose metabolism *(Lu et al., 2010)* • Up-regulated in insulin-resistant heart and adipose tissue of T2DM patients *(Lu et al., 2010)* • Represses cholesterol biosynthesis enzymes and inhibits cholesterol biosynthesis by targeting SR-BI *(Vickers et al., 2014; Wang et al., 2013a)*
miR-375	**IGF1R** **PDK1** **p53**	• Incorporation and transport by HDL particles *(Rottiers and Naar, 2012)* • Increased in serum of T2DM patients (biomarker for T2DM, potential pharmacological target) *(Higuchi et al., 2015; Villard et al., 2015)* • Increased in serum and tissues of obese mice *(Higuchi et al., 2015)* • Regulator of insulin secretion *(Poy et al., 2004)*

let-7b	**INSR** **IRS2** **IGF1R**	• Important role in glucose metabolism *(Zhu et al., 2011)* • Downregulated in the circulation in diet-inuced obesity in mice *(Hsieh et al., 2015)* • Over-expression leads to insulin resistance and impaired glucose tolerance *(Zhu et al., 2011)* • Increased during adipocytic differentiation, regulates adipogenesis *(Sun et al., 2009)*
miR-192	**Zeb1/2** **SLC39A6** **RB1**	• Increased in models of Diabetic Nephropathy and in kidneys from humans with chronic kidney disease *(Ma et al., 2016)* • Increased in prediabetic patients and in early stages of DN *(Jia et al., 2016; Parrizas et al., 2015)* • Circulating miR is high diagnostic biomarker for NAFLD and is increased in glucose intolerant mice *(Becker et al., 2015)*
miR-194	**AGK** **YAP-1**	• Inhibits the PI3K/Akt/FoxO3a signaling pathway *(Chi, 2015)* • HNF1a induces its expression *(Krutzfeldt et al., 2012)* • When downregulated in skeletal muscles induces insulin-stimulated glucose uptake *(Latouche et al., 2016)* • Reduced expression in pre-diabetic and diabetic skeletal muscles *(Latouche et al., 2016)*
miR-193b	**FASN** **SMAD3** **CREB5**	• Increased in prediabetic patients and in early stages of DN *(Jia et al., 2016; Parrizas et al., 2015)* • Controls adiponectin production in human white adipose tissue *(Belarbi et al., 2015)*

iv) Salt Inducible Kinase 1

Salt Inducible kinase 1 (Sik1) is a serine/threonine protein kinase firstly identified as an induced kinase in adrenal glands of rats fed with a high-salt diet (Wang et al., 1999) and belongs to the family of AMP-activated protein kinases (AMPKs). Sik1 is normally located in the nucleus and when phosphorylated by Protein kinase A (PKA) upon cAMP stimulus, it is translocated to the cytoplasm. It is involved in a variety of

processes including cell cycle regulation, gluconeogenesis and lipogenesis regulation (Katoh et al., 2004; Patel et al., 2014).

A recent study revealed that Sik1 plays a crucial role in regulating the activity of SR-BI in adrenals (Figure 8) (Hu et al., 2015). To be more specific, it was found that Sik1 interacts with and phosphorylates the Ser496 in the C-terminal domain of SR-BI thus enhancing the selective transport of CE from HDL into the adrenals. Additionally, another study has revealed that Sik1 inactivates SREBP-1c, the master regulator of lipogenic genes, therefore inhibiting *de novo* lipogenesis in liver (Figure 9) (Yoon et al., 2009).

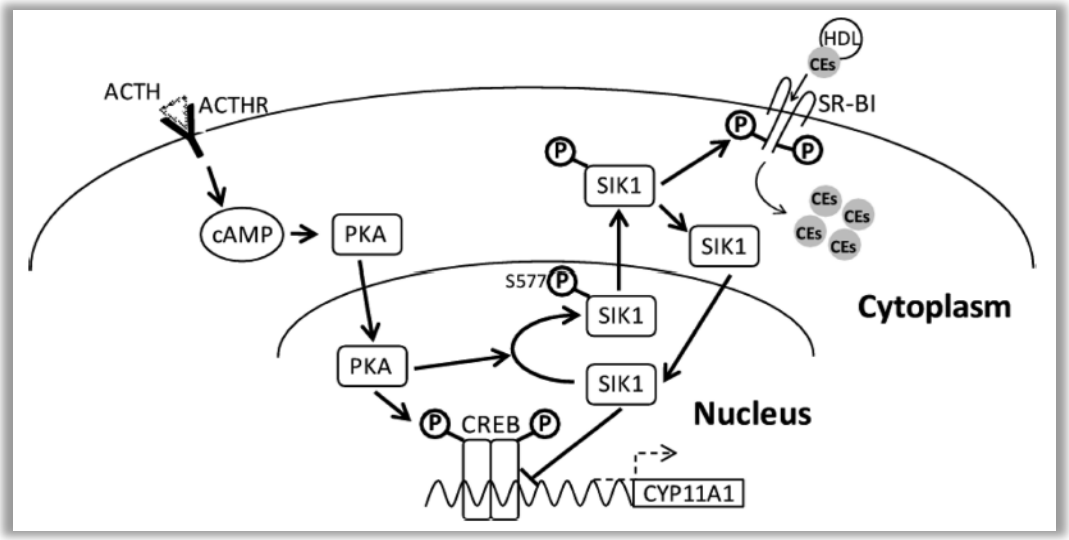

Figure 8. The stimulatory role of Sik1 in the selective CE uptake through SR-BI in adrenals (Hu et al., 2015).

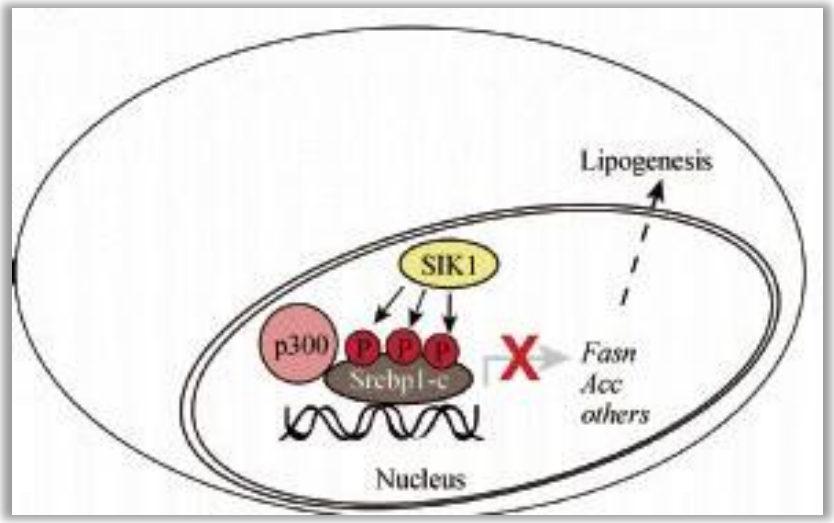

Figure 9. The regulation of SREBP1-c by Sik1 in the liver (BERDEAUX, 2011).

AIM OF THE STUDY

In this study we wanted to identify novel differentially expressed genes and microRNAs in a mouse model of the Metabolic Syndrome in order to unravel new regulatory mechanisms being involved. Furthermore, we pursued to identify alterations in the expression levels of several microRNAs in mice with Metabolic Syndrome and Type II diabetes that could be used as clinical biomarkers of these diseases.

MATERIALS AND METHODS

Mouse models

ApoE3L.CETP transgenic mice

In order to study the Metabolic Syndrome, a specific animal model that mimics the human disease state has been created. The translational model for MetS is the APOE*3Leiden.humanCholesteryl Ester Transfer Protein (E3L.CETP) transgenic mouse (van den Hoek et al., 2014) that has been obtained by cross-breeding the E3L mice (they exhibit a human-like lipoprotein metabolism) with the human CETP-expressing mice (CETP enzyme mediates the transfer of triglycerides (TGs) from TG-rich lipoproteins to HDL and LDL particles in exchange for cholesteryl esters) (Sandhofer et al., 2006). This model has already been used in terms of research concerning hyperlipidemia and atherosclerosis (Westerterp et al., 2006; Zadelaar et al., 2007) and since it mimics the human disease state, this model provides the opportunity to examine several responses and features upon both lipid-lowering and HDL-raising conditions. Upon HFD, these mice manifest the features of metabolic syndrome and especially after a 12 week time period. This fact gives the opportunity to monitor and identify changes in gene expression throughout the progression of the disease.

Expression of ApoE3Leiden and human CETP gene in mice affects the metabolism of plasma lipoproteins and mimics the human lipoprotein profile (Figure 10). Chylomicrons secreted from the intestine and VLDL particles secreted from the liver, form remnant particles after LPL mediated lipolysis in the circulation. ApoE on such particles mediates their uptake in the liver by the LDLr. However, clearance of apoB-containing particles via the LDLr pathway is attenuated in mice expressing the mutated form of human APOE gene, APOE3Leiden. In contrast to humans, mice do not express the cholesteryl ester transfer protein (CETP) which exchanges cholesteryl esters with triglycerides between HDL and VLDL/LDL. Thus, by inserting the hCETP gene in ApoE3Leiden mice results in high levels of VLDL/LDL-C and relatively low levels of HDL-C.

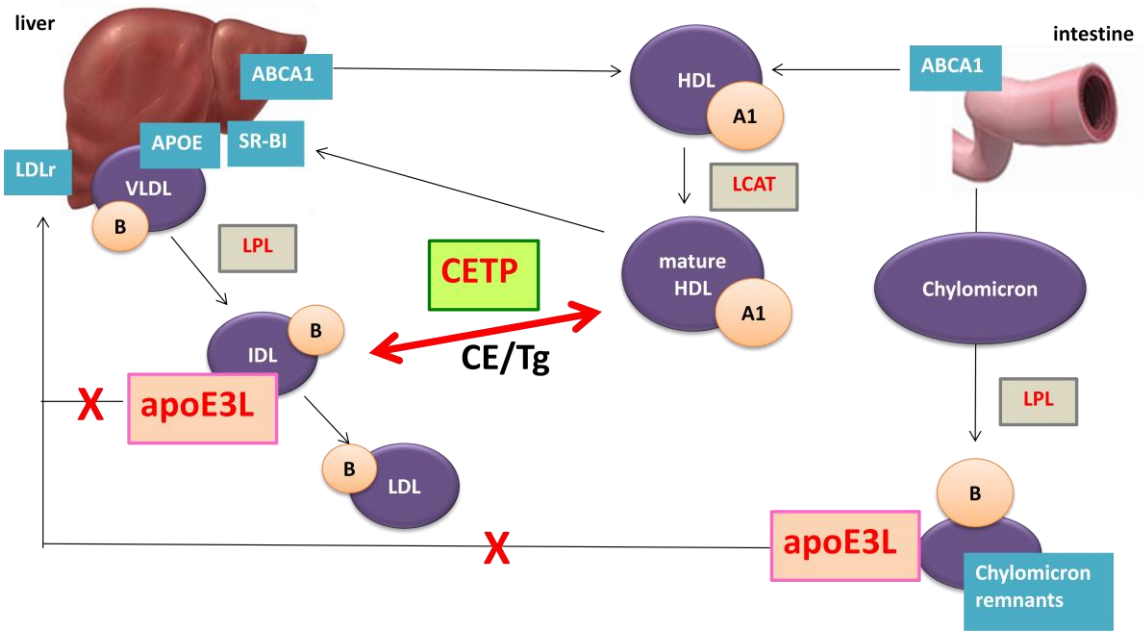

Figure 10. Expression of the mutated ApoE3Leiden and hCETP gene in mice lead to a human like phenotype

In this study, we analyzed mice that were fed with different diets (high-fat diet/HFD and low-fat diet/LFD) in order to observe the expression levels of several genes and microRNAs in the liver as well as the presence of specific microRNAs in the circulation. Furthermore we wanted to monitor their potential changes due to the dietary habits in several time points of the disease progression. Moreover, we performed a bioinformatic-based search in order to identify potential target genes of our selected microRNAs (using the online tools miRDB, TargetScan and miRanda) and tried to correlate their expression levels with alterations in several genes that were identified deregulated in liver microarrays of the same mice. Our last goal was to unravel new regulatory mechanisms that have a distinct role in the pathogenesis of Metabolic Syndrome. To be more specific, 3 month-old male mice were fed with the specific diet for 4, 8, 12 and 16 weeks as depicted in the figure (Figure 11).

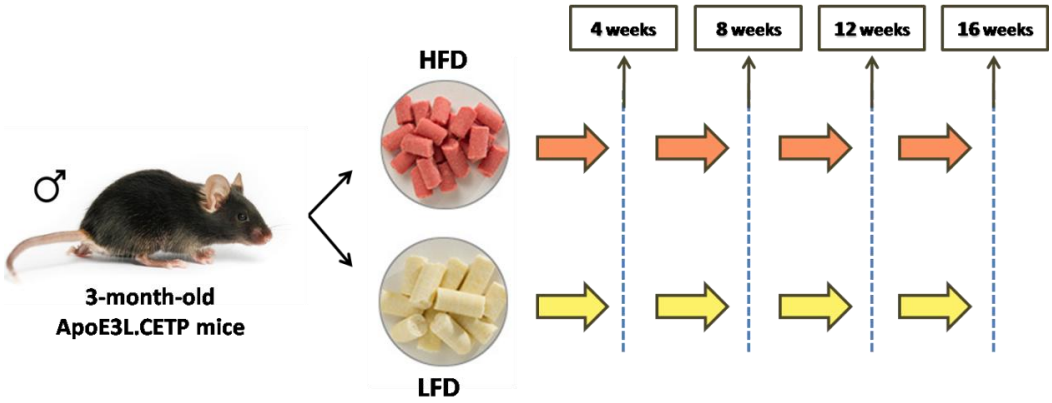

Figure 11. 3-month-old ApoE3L.CETP mice were fed either a High Fat Diet (HFD) or a Low Fat Diet (LFD) and after specific time points (4, 8, 12 and 16 weeks of diet) were sacrificed.

Genotyping of APOE3L mice - DNA extraction / PCR for ApoE3L transgene

The DNA extraction was carried out from mouse tails which were initially incubated overnight or for 4-5 hours at 55°C in tail buffer with Proteinase K. The solution that was used is prepared by adding 5μL of PK (10mg/mL) in 495μL tail buffer for each sample. DNA extraction was performed by following the Phenol-Chloroform protocol and the ApoE3L gene was detected by performing PCR (Table 2, Figure 12). PCR products were subjected to electrophoresis in a 2% agaroze gel.

Table 2. PCR reaction for the detection of ApoE3L transgene

PCR for ApoE3L	
Reagent	**Volume (μL)**
Nuclease free water	13.8
$MgCl_2$	1.7
dNTPs (2mM)	2.5
Buffer Taq 10x (Minotech)	2.5
Taq polymerase (Minotech)	0.4
ApoE3L FW primer (10μM)	1
ApoE3L REV primer (10μM)	1
Genomic DNA	1
Final Volume	24

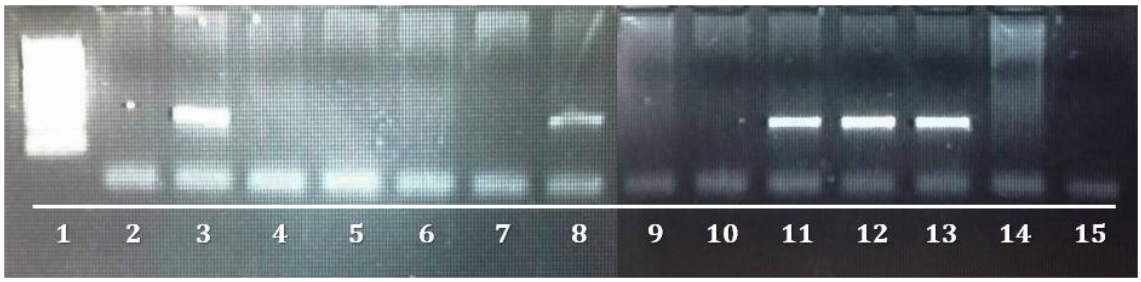

Figure 12. Genotyping. (1): ladder (λ DNA-BstEII Digest, NEB), (2, 4, 5, 6, 7, 9, 10): non transgenic mice, (3, 8, 11, 12): transgenic mice, (13): positive control of *APOE*3Leiden* gene, (14): negative control (C57BL/6 mouse DNA), (15): blank

Akt2$^{-/-}$ mice

A model that is widely used and already described to exert a Diabetes Mellitus-like syndrome is the mouse lacking the Akt2 protein kinase/PKBβ (Akt2$^{-/-}$) (Cho et al., 2001; Garofalo et al., 2003). Akt2/PKBβ is an intermediate in the glucose-signaling pathway which controls glucose uptake both in muscle and fat tissue as well as gluconeogenesis in the liver (Kohn et al., 1996; Liao et al., 1998; Ueki et al., 1998). Several studies indicate that mice lacking Akt2 are prone to be diabetic. To be more specific, it has been found that siRNA-silencing of Akt2 results in a diminished insulin-stimulated glucose uptake (Katome et al., 2003). Furthermore, Akt2$^{-/-}$ mice exhibit impaired glucose tolerance and simultaneously suffer from insulin resistance, elevated triglycerides and hyperglycemia (Garofalo et al., 2003; Jiang et al., 2003), meaning that Akt2 represents a crucial kinase for glucose metabolism. In our study we measured the blood glucose levels of Akt2$^{-/-}$ male mice (non-starved) to verify that they exert a Diabetes-like syndrome and we analyzed the expression of microRNAs in their sera and livers at different time points (6 and 12 weeks-old). C57BL6/J mice were used as the wild type control group.

Blood glucose measurment

Blood glucose levels in mice were measured using the TRUE Result device and the respective strips by applying one blood droplet from mouse tails.

Hepatic cell lines

HEPA (murine) and HepG2 (human) hepatic cell cultures were used to identify the expression of specific microRNAs and for subsequent transfection experiments. Cells were cultured in high glucose Dulbecco's modified Eagle's medium (DMEM) with 10% fetal bovine serum (FBS), and penicillin/streptomycin (P/S) at 37^{o}C in a 5% CO_2 incubator.

Blood collection and serum isolation

Initially, our mice were anesthetized with isoflurane and their blood was collected directly from their hearts by using disposable syringes. After 30 minutes at room temperature (RT) on bench, the collected bloods were centrifuged twice, at 3000 rpms/4^{o}C for 20 minutes each time, in order to obtain the serum as pure as possible. Lastly, the isolated sera were stored at -80^{o}C.

Tissue collection

After blood collection, mice were subjected to anatomy and collection of specific tissues such as liver, adipose tissue, pancreas, heart, small intestine, large intestine, kidneys and adrenals. In this project, we analyzed livers from the two mouse strains.

microRNA isolation from serum

In order to isolate the total microRNAs from mice sera we used the miRCURY RNA Isolation Kit by EXIQON (Product No.: 300112) according to manufacturer's protocol. The final volume of serum that was analyzed from each mouse was 50μl. Spike-in template (provided by the kit) was added every time (1μL) in each serum sample and was used as the reference microRNA. The previous step is crucial because none microRNA is known to be expressed consistently at basal levels in the circulation. On the other hand, 5S ribosomal RNA was used as reference for microRNAs in the liver. The concentrations of the isolated miRNAs were measured at the TECAN Infinite 200® PRO instrument and if needed they were diluted to the appropriate volume of nuclease-free water at concentrations shown in Tables 4 and 5. miRNAs were further subjected to cDNA synthesis.

RNA extraction from tissues/cells

Total RNA (including microRNAs) was extracted from hepatic cell lines and mouse livers using the RNAiso Plus reagent (#9109, Takara) according to the manufacturer's protocol. Cells were initially lysed while liver tissues were homogenized. Extracted RNA was diluted in 100μL of Nuclease Free Water and its concentration and purity was measured at TECAN Infinite 200® PRO instrument.

cDNA synthesis from total RNA (from tissues and cell lysates)

In order to synthesize cDNAs by RNA isolated from liver or hepatic cell cultures (HEPA, HepG2) we used the M-MLV Reverse Trancriptase (Invitrogen, #28025). The RNA samples were prepared in a concentration of 200ng/μL and the reaction setup was the following:

Table 3. cDNA synthesis reaction using RNA template isolated from mouse liver and hepatic cell lines

cDNA synthesis (M-MLV reverse transcriptase)	
Reagent	**Volume (μL)**
Nuclease-free water	20
dNTPs (2mM)	5
Random primers (#3801, Takara)	3
Template total RNA (200ng/μL)	5
DTT (0.1M)	5
First Strand buffer (5x)	10
RNase OUT Recombinant Ribonuclease Inhibitor (#10777019, Invitrogen)	1
M-MLV reverse transcriptase (200U/μL)	1
Final Volume	50

cDNA synthesis from microRNAs (from tissues, cell lysates and serum)

In order to synthesize the cDNAs from circulating (serum) or hepatic microRNAs (hepatic cell lines, liver tissues) we used the Universal cDNA Synthesis Kit II by EXIQON (Product No.: 203301) and the working solution for each sample is shown in Tables 4 and 5. Afterwards, the synthesized cDNA was diluted either 1:20 (circulating microRNAs) or 1:8 (liver microRNAs) and then used for RT-PCR.

Tables 4, 5. cDNA synthesis working solutions per sample

cDNA synthesis (circulating microRNAs)	
Reagent	**Volume (μL)**
5x Reaction buffer	2
Nuclease-free water	3
Enzyme mix	1
Template total RNA (5ng/μL)	4
Final Volume	10

cDNA synthesis (liver microRNAs)	
Reagent	**Volume (μL)**
5x Reaction buffer	2
Nuclease-free water	5
Enzyme mix	1
Template total RNA (100ng/μL)	2
Final Volume	10

qRT-PCR for microRNAs

As we have already mentioned, we have the predominant miRNA (miRNA) and the opposite sequence (miRNA*) produced from each precursor miRNA. By searching in miRBase we found the predominant sequence for each circulating miRNA and then we obtained the specific primers for their identification (Table 5). The primers were received lyophilized, they were re-suspended in 220μL of nuclease-free water and stored in aliquots at -20^{o}C.

Table 6. Primers (EXIQON) used in the qPCR experiments and their target sequences

miRNA	Primer Set by EXIQON	Target Sequence
miR-27a	hsa-miR-27a-3p LNA™ PCR primer set, UniRT (Product No.: 206038)	UUCACAGUGGCUAAGUUCCGC
miR-130b	hsa-miR-130b-3p LNA™ PCR primer set, UniRT (Product No.: 204317)	CAGUGCAAUGAUGAAAGGGCAU
miR-135a	hsa-miR-135a-5p LNA™ PCR primer set, UniRT (Product No.: 204762)	UAUGGCUUUUUAUUCCUAUGUGA
miR-192	hsa-miR-192-5p LNA™ PCR primer set, UniRT (Product No.: 204099)	CUGACCUAUGAAUUGACAGCC
miR-193b	mmu-miR-193b-3p LNA™ PCR primer set, UniRT (Product No.: 205062)	AACUGGCCCACAAAGUCCCGCU
miR-194	hsa-miR-194-5p LNA™ PCR primer set, UniRT (Product No.: 204080)	UGUAACAGCAACUCCAUGUGGA
miR-223	hsa-miR-223-3p LNA™ PCR primer set, UniRT (Product No.: 205986)	UGUCAGUUUGUCAAAUACCCCA
miR-375	hsa-miR-375 LNA™ PCR primer set, UniRT (Product No.: 204362)	UUUGUUCGUUCGGCUCGCGUGA
let-7b	hsa-let-7b-5p LNA™ PCR primer set, UniRT (Product No.: 204750)	UGAGGUAGUAGGUUGUGUGGUU

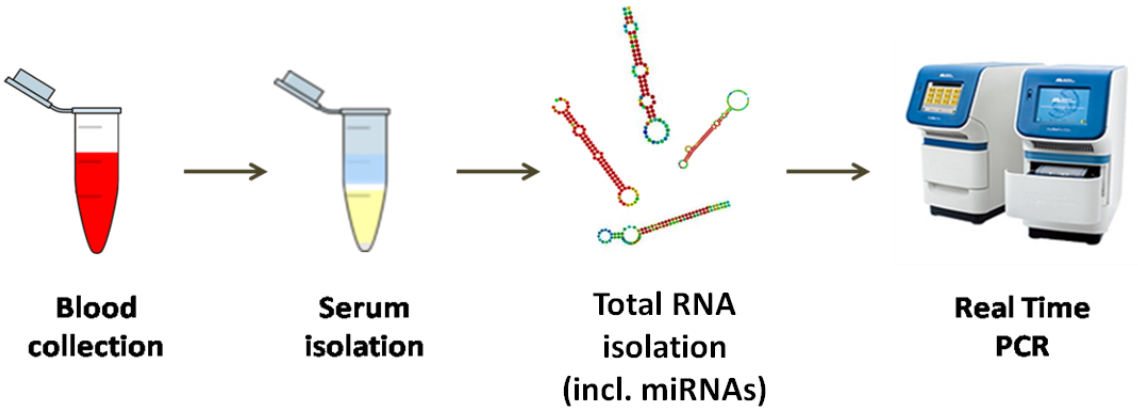

Figure 13: The experimental procedure followed for the identification and quantification of circulating microRNAs

The diluted cDNAs were used for Real Time PCR analysis using the ExiLENT SYBR® Green master mix by EXIQON (Product No.: 203403) and the respective primers for each miRNA, as shown in Tables 7 and 8:

Tables 7 and 8. Real time PCR working solutions per sample

Real Time PCR (for circulating microRNAs)	
Reagent	**Volume (μL)**
PCR master mix	5
PCR primer mix	1
Diluted cDNA template (1:20)	4
Final Volume	10

Real Time PCR (for liver microRNAs)	
Reagent	**Volume (μL)**
PCR master mix	5
PCR primer mix	1
Diluted cDNA template (1:8)	4
Final Volume	10

qRT-PCR for mRNA analysis – Validation experiments of microarrays

qPCR experiments were performed in order to validate the findings of liver transcriptomic analysis done in APOE3L.CETP fed either a HDF or a LFD. Specific primers were designed for selected genes by using the DNASTAR and Fast PCR programs as following:

Table 9. Primers designed for validation qPCR experiments of differentially expressed genes in livers of APOE3L.CETP mice

Gene	Primers sequence
Orm3	**Fwd:** 5'-CGCTAGAAGGCCAGATATCCC-3' **Rev:** 5'-ACTGCACCTGTCCTTTTTCCA-3'
Pparg	**Fwd:** 5'-TCACAATGCCATCAGGTTTGG-3' **Rev:** 5'-CTGGGTTCAGCTGGTCGATA-3'
Lepr	**Fwd:** 5'-AGCCTATACGCTTGTCATGGAT-3' **Rev:** 5'-TTCGTCAGGGGCTTCCAAA-3'
Sik1	**Fwd:** 5'-GACACCATTGCTGACCAGGAA-3' **Rev:** 5'-GGCAGTCCAGGAGGTCTGTAGT-3'
Cyp7a1	**Fwd:** 5'-AATCTACCCAGACCCTTTGAC-3' **Rev:** 5'-AAGGTGGTCTTTGCTTTCCCA-3'
Sqle	**Fwd:** 5'-TGGAGGCCTCTCAGAATGGT-3' **Rev:** 5'-TAAGGACGCCTCGTTTGTTC-3'
Fasn	**Fwd:** 5'-CCATGGCAGCTGTTGGTTTG-3' **Rev:** 5'-GTGTCCTCAGAGTTGTGGCA-3'
Pcsk9	**Fwd:** 5'-TATAGCCGCATCCTCAACGC-3' **Rev:** 5'-CCCGACTGTGATGACCTCTG-3'
Saa1	**Fwd:** 5'-GACACCATTGCTGACCAGGAA-3' **Rev:** 5'-GGCAGTCCAGGAGGTCTGTAGT-3'
Saa3	**Fwd**: 5'-CTGTTCAGAAGTTCACGGGAC-3' **Rev:** 5'-AGCAGGTCGGAAGTGGTT-3'

Cloning of Sik1 3' UTR

Specific primers were designed with DNA STAR and Fast PCR programs (Table 10) for PCR amplification of the 3'UTR of Sik1 by using mouse genomic DNA as a template. AmpliTaq Gold 360 Master mix (Applied Biosystems) was used for the PCR reaction (Table 11) and the fragment was subsequently cloned into the XbaI site of the pGL3promoter vector (Promega, Figure 15). A BamHI site was introduced in the forward primer in order to identify the correct orientation of the insert.

Table 10. Primers designed for validation amplification of Sik1 3' UTR in pGL3 promoter vector. *XbaI* (TCTAGA), *BamHI* (GGATCC)

Name	Primers sequence
Sik1-3'UTR-Fwd	5'- TGCTCTAGA GGATCCGAGGCGTGATGAGCTGGG -3'
Sik1-3'UTR-Rev	5'- ACGAGATCTATGCCGTTTGTCTTCCCCTG -3'

Table 11. PCR reaction for amplification of Sik1 3'UTR fragment

PCR reaction for amplification		
Reagent	**Small scale (25µL)**	**Large scale (50µL)**
Nuclease free water	10	20
AmpliTaq Gold Master mix	12.5	25
Forward primer (10µM)	0.5	1
Reverse primer (10µM)	0.5	1
Template DNA	1.5	3

PCR clean up

The PCR product (Sik1 3'UTR fragment) was cleaned up using NucleoSpin® Gel and PCR Clean-up kit from MACHEREY-NAGEL according to the respective protocol.

Digestions of pGL3 promoter vector

The pGL3 promoter was digested with restriction enzymes: a) XbaI (NEB) and b) HindIII / KpnI (NEB) that give one linear fragment of 5010bp and two fragments of 4770bp and 240pb respectively, according to the vector map (Figure 14).

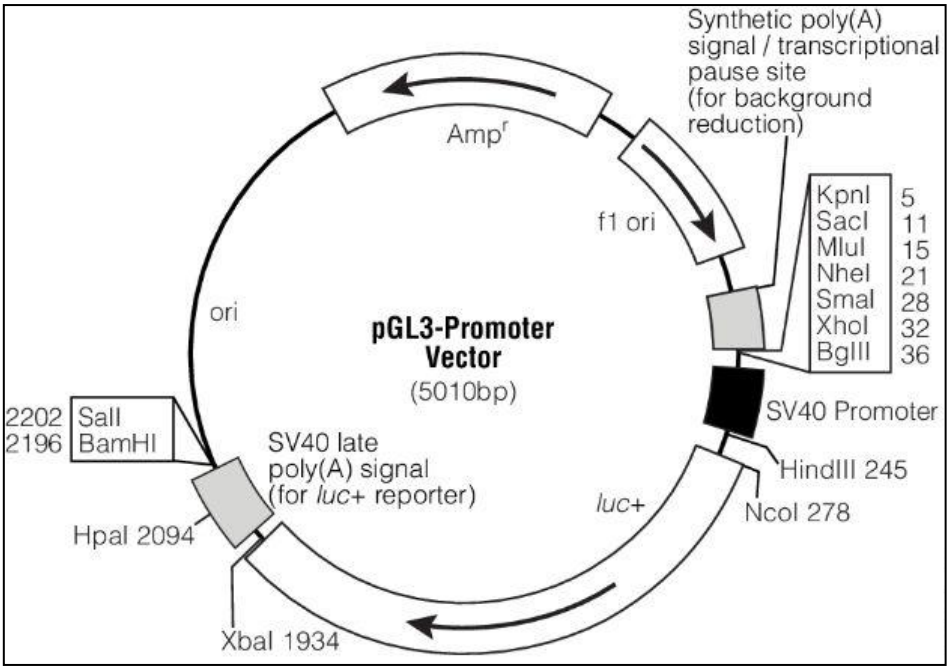

Figure 14. pGL3 promoter vector used for cloning of the Sik1 3' UTR.

Tables 12 and 13. Digestion reactions of pGL3 promoter vector with XbaI and HindIII/KpnI

Digestion of pGL3 promoter vector	
Reagent	**Volume (µL)**
Nuclease-free water	15
Cut Smart buffer 10x (#B7204S, NEB)	2
XbaI (20.000 U/mL, NEB)	1
pGL3 promoter vector (0,5µg/µL)	2
Final Volume	20

Digestion of pGL3 promoter vector	
Reagent	**Volume (µL)**
Nuclease-free water	15
Cut Smart buffer 10x (#B7204S, NEB)	2
HindIII (20.000 U/mL, NEB)	0.5
KpnI (10.000 U/ mL, NEB)	0.5
pGL3 promoter vector (0,5µg/µL)	2
Final Volume	20

Ligation reaction

Prior to the ligation reaction both pGL3 promoter vector and the insert were digested with XbaI (Tables 13, 14) in order to obtain complementary ends for subsequent ligation. The restriction reactions were performed at 37°C for 1 hour, both followed by heat inactivation of the enzyme at 65°C for 20 minutes. Furthermore, the

free phosphorylated ends of the restricted vector were dephosphorylated to avoid self-ligation of the vector using Antarctic phosphatase (#B0289S, NEB) in a reaction at 37 ^{o}C for 15 minutes, followed again by heat inactivation of the enzyme at 65^{o}C for 20 minutes.

Tables 14 and 15. Digestion reactions of pGL3 promoter vector and insert with XbaI

Digestion of pGL3 promoter vector with XbaI	
Reagent	**Volume (µL)**
Nuclease-free water	24
Cut Smart buffer 10x (#B7204S, NEB)	3
XbaI (20.000 U/mL, NEB)	1
pGL3 promoter vector (0,5µg/µL)	2
Final Volume	30

Digestion of insert with XbaI	
Reagent	**Volume (µL)**
Nuclease-free water	7.5
Cut Smart buffer 10x (#B7204S, NEB)	9
XbaI (20.000 U/mL, NEB)	0.5
Insert Sik1 3'UTR fragment (50ng/µL)	73
Final Volume	90

The ligation reaction was performed at 4^{o}C overnight and the reaction setup was the following:

Table 16. Ligation reaction between pGL3 (restricted by XbaI) and Sik1 3'UTR (restricted by XbaI)

Ligation Reaction	
Reagent	**Volume (μL)**
Nuclease-free water	4
T4 Ligase buffer 10x (Invitrogen)	1
T4 Ligase (Invitrogen)	1
pGL3 promoter vector	1
Sik1 3'UTR insert	3
Final Volume	10

Transformation

DH10β competent bacteria were transformed either with the pGL3-Sik1-3'UTR vector or with the self-ligated vector. 100μL of bacteria cells were transferred to each tube containing the above vectors, and after 30 minutes on ice they were heat-shocked at 42^{o}C for 45 seconds. 900mL of LB medium were added in each tube and bacteria were incubated at 37^{o}C for 1 hour. Afterwards, the cells were centrifuged, redissolved at 100μL final volume of LB, poured in petri dishes and let to develop colonies at 37^{o}C overnight. The following day, 15 distinct bacteria colonies were inoculated in 2mL LB medium and let to proliferate at 37^{o}C overnight under shaking.

Minipreps

Plasmid isolation and purification from the 15 bacteria colonies with pGL3-Sik1-3'UTR vector were performed by using the NucleoSpin® Plasmid kit (MACHEREY-NAGEL) according to the manufacturer's protocol. Plasmid DNAs were measured at TECAN Infinite 200® PRO instrument and afterwards they were subjected to restriction digestion with BamHI as following:

Table 17. Restriction digestion of purified plasmid DNAs with BamHI

Restriction of plasmid DNAs	
Reagent	**Volume (µL)**
Nuclease-free water	11
BamHI (NEB)	0.5
Cut Smart buffer 10x (NEB)	1.5
Plasmid DNA (1µg/µL in total)	2
Final Volume	15

RESULTS - DISCUSSION

i) Identifying circulating miRNA levels in APOE3L.CETP and Akt2$^{-/-}$mice

Initially, we tried to monitor the levels of circulating miRNAs throughout the progression of Metabolic Syndrome. For this reason, we analyzed the serum of APOE3L.CETP mice fed with a HFD diet for 4, 8, 12 and 16 weeks in order to specify potential alterations in miRNA levels (Figure 15). As a control group we used mice fed with a LFD for the same time periods. Data were analyzed by using the ΔCτ parameter which refers to the cycle of the Real Time PCR amplification where we can observe an increase in the copy numbers of the cDNAs. The smaller the ΔCτ, the more abundant the miRNA is in the serum and conversely when ΔCτ is high, the miRNA levels are low.

We can observe from the graphs of Fig. 15 that in a 4 week diet intervention (panel A) no changes occur in circulating miRNA profile but as the disease progresses, several miRNAs present altered levels. More specifically, in 8 weeks of HFD (Panel B), miR-135a and miR-375 were found to be decreased in the serum while in the 12-week HFD group (panel C) miR-27a, miR-130b and miR-193b appeared to be significantly increased. After 16 weeks diet intervention (panel D), only miR-135a was upregulated in HFD-fed mice, but still we could not have a clear case due to the small number of mice analysed.

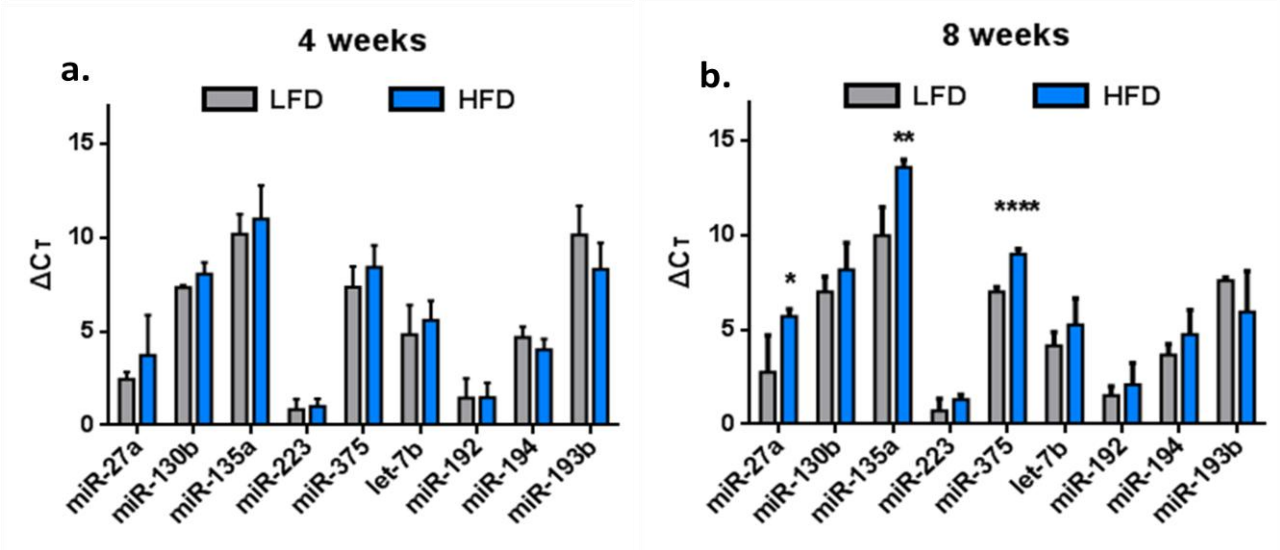

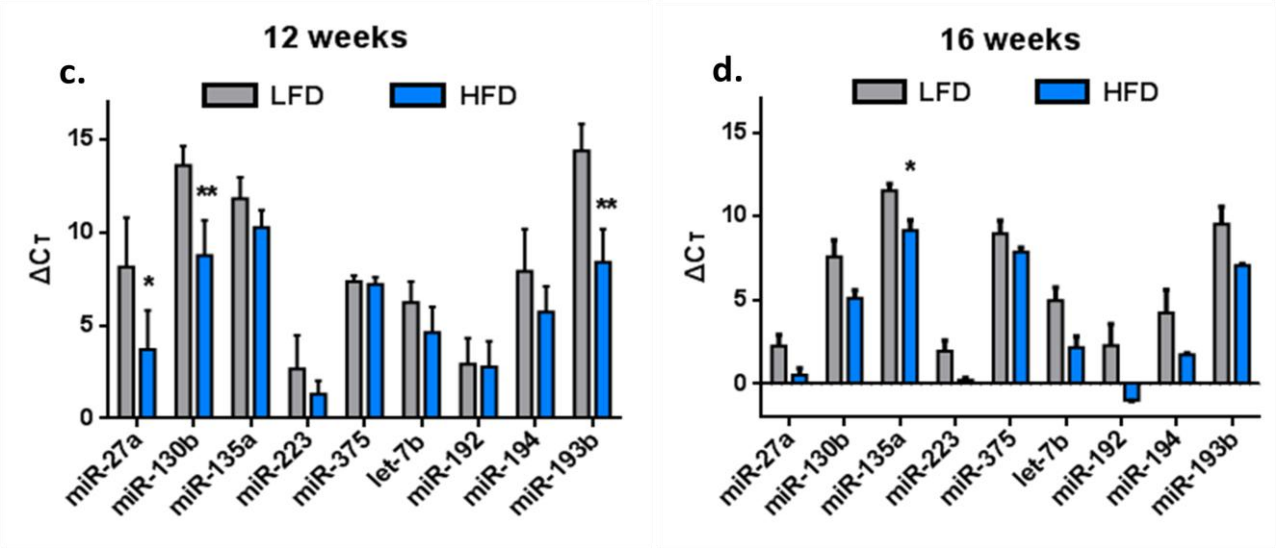

Figure 15: Circulating microRNA levels in the serum of HFD-fed (blue bars) versus LFD-fed (grey bars) ApoE3L.CETP mice. Data is shown as ΔCτ. All values represent the mean ± S.D (**a.** 4 weeks: N=3 LFD, N=4 HFD, **b.** 8 weeks: N=4 LFD, N=4 HFD, **c.** 12 weeks: N=3 LFD, N=6 HFD **d.** 16 weeks: N=2 LFD, N=2 HFD). Student's t-test was performed. **P*<0.05, ***P*<0.01, ****P*<0.001, *****P*<0.0001.

MiR-135a has already been found to suppress adipogenesis by inhibiting the Wnt signalling pathway (Chen et al., 2014), so its decrease in the circulation of 8 weeks HFD-fed mice could be correlated with the development of the extended adipose tissue that these mice present, which eventually become obese. However, its levels are increased after a 12 week diet intervention, a fact that could be attributed to a response mechanism of these mice in order to inhibit further adipogenesis.

MiR-375 has already been characterized as a biomarker of T2DM and has been also found increased in the circulation and in tissues of obese mice (Higuchi et al., 2015; Villard et al., 2015). In contrast, we observe here that its levels in the serum of 8-weeks HFD diet-fed mice present a serious reduction, which could possibly suggest the presence of an internal regulatory mechanism that tries to inhibit the onset of Metabolic Syndrome. However, after a 12-week diet intervention, no changes in the levels of circulating miR-375 can be identified.

Interestingly, we found that the circulating levels of miR-27a and miR-130b were increased in the 12-weeks HFD-fed, a time point where the disease has been fully developed. These results are in agreement with previous observations showing that miR-

27a is upregulated in the circulation of MetS patients (Karolina et al., 2012) and miR-130b levels are increased in the circulation of obese mice (Wang et al., 2013b), while simultaneously both miRs constitute a risk factor for MetS.

Moreover, the increase in the levels of miR-193b could be attributed to the diabetic parameters of MetS as this specific miR has been found increased in prediabetic patients and in patients at early stages of Diabetic Nephropathy (Jia et al., 2016; Parrizas et al., 2015).

Subsequently, we wanted to examine the expression levels of these circulating miRNAs in the context of T2DM, using the diabetic Akt2$^{-/-}$ mouse model. For this set of experiments we used animals with ages ranging from 6 to 12 weeks, and the comparisons were made with age-matched C57BL6/J mice.

Firstly, to validate that the Akt2$^{-/-}$ mice exert a diabetic phenotype, blood glucose levels were measured in non-fasting conditions prior to blood collection and miRNA isolation (Figure 16a). By analyzing the serum of these mice, we found that circulating miR-192 and miR-194 were strongly upregulated only in the diabetic Akt2$^{-/-}$ mice, while miR-223 levels were also slightly elevated (Figure 16b).

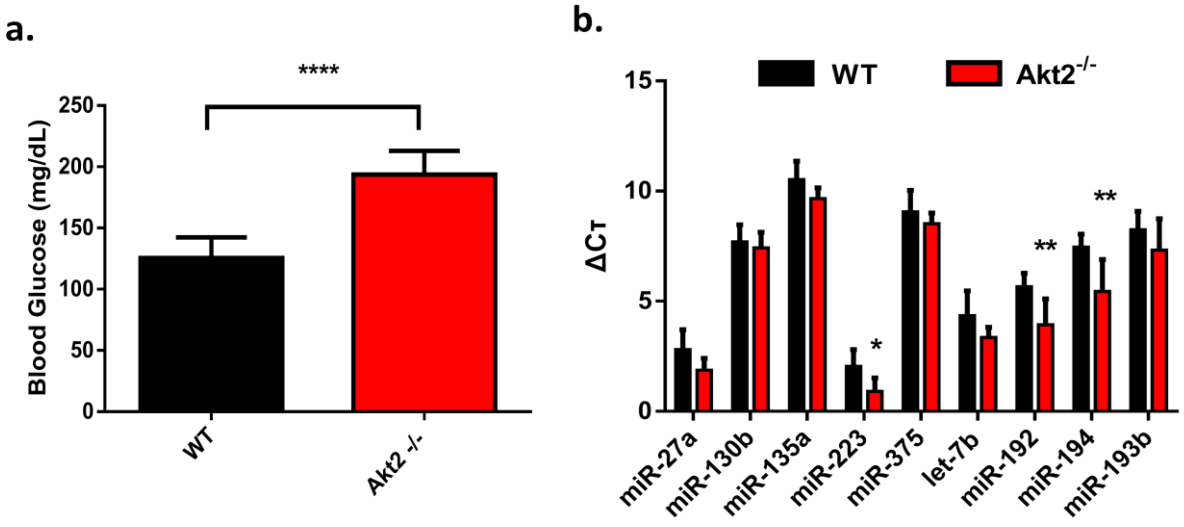

Figure 16: **a.** Blood glucose levels and **b.** circulating miRNA levels in Akt2$^{-/-}$ (N=7, red bar) versus WT (N=7, black bar) mice. Data is shown as ΔCτ. All values represent the mean ± S.D. Student's t-test was performed. *P<0.05, **P<0.01, ***P<0.001, ****P<0.0001.

Increased levels of miR-192 have already been associated with prediabetes and the early stages of Diabetic Nephropathy in humans (Jia et al., 2016; Parrizas et al., 2015) but also with glucose intolerance in mice (Becker et al., 2015), findings that strengthen our observations. On the other hand, miR-194 levels were recently shown to be decreased in pre-diabetic and diabetic skeletal muscles (Latouche et al., 2016). The fact that we observe a clear increase in its circulating levels is quite contradictory, but we could hypothesize that miR-194 could possibly exert its regulatory role in other tissues.

As far as miR-223 is concerned, previous research showed an upregulation of this miR in insulin-resistant heart and adipose tissue of T2DM patients (Lu et al., 2010) and here we show an elevation of its circulating levels in diabetic mice. Several studies indicate that during the pathogenesis of Type II Diabetes there is an ongoing cytokine-driven acute-phase inflammation, which is depicted in elevated levels of specific inflammatory markers such as IL-6 and C-reactive protein (Barzilay et al., 2001; Festa et al., 2002; Schmidt et al., 1999). Furthermore, miR-223 has also been found to be implicated in the regulation of inflammation (e.g negative regulator of TLR-triggered inflammatory cytokines, (Zhuang et al., 2012)) and since its circulating levels are increased in the diabetic mice we could hypothesize that miR-223 exerts a potential anti-inflammatory role.

ii) Studying the miRNA expression levels in the livers of 12 weeks HFD-fed APOE3L.CETP and Akt2$^{-/-}$ mice

Subsequently, we wanted to investigate whether miR-27a and miR-130b, that were found increased in the circulation of 12-weeks HFD-fed APOE3L.CETP mice, were also highly expressed in the liver (Figure 17).

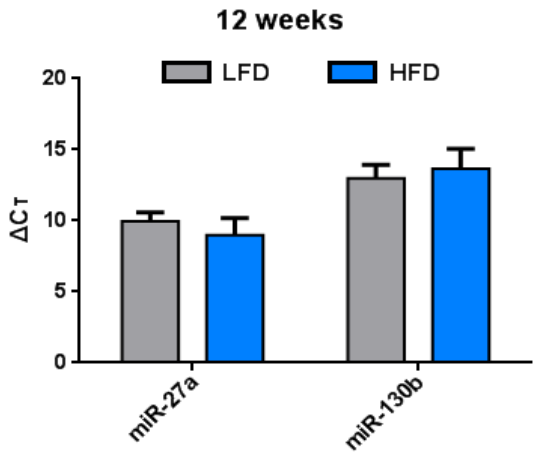

Figure 17: Expression analysis of miR-27a and miR-130b in liver tissues of 12 weeks HFD-fed (N=5, blue bars) versus LFD-fed (N=3, grey bars) APOE3L.CETP mice. Data is shown as ΔCτ. All values represent the mean ± S.D. Student's t-test was performed. **P*<0.05, ***P*<0.01, ****P*<0.001, *****P*<0.0001.

We observed a slight increase in the expression levels of miR-27a in the liver, yet not statistically significant, while no change was observed in the hepatic expression of miR-130b.

Furthermore, we studied the hepatic expression levels of miR-192 and miR-194 that were found to be increased in the circulation of diabetic mice and we observed only a slight elevation on their expression, but again not statistically significant.

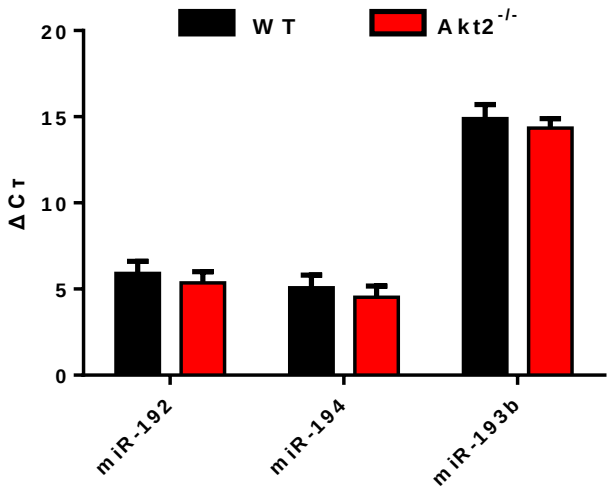

Figure 18: Expression analysis of miR-192, miR-194 and miR-193b in livers of Akt2$^{-/-}$ (N=4, red bar) versus WT (N=4, black bar) mice. Data is shown as ΔCτ. All values represent the mean ± S.D. Student's t-test was performed. **P*<0.05, ***P*<0.01, ****P*<0.001, *****P*<0.0001.

iii) Identifying differentially expressed hepatic genes in 12-weeks HFD-fed APOE3L.CETP mice

Transcriptomic analysis (Affymetrix) in the livers of ApoE3L.CETP mice that was performed in our lab revealed significant changes in the expression levels of several genes involved in lipid and glucose metabolism (Table 18) and this was even more profound in the 12 weeks HFD time point, where the syndrome is fully developed. For this reason we wanted to validate these findings by performing RT-qPCR analysis experiments for selected up- and down-regulated genes shown in Table 18.

Table 18: Differentially expressed genes in the liver of 12-weeks HFD-fed APOE3L.CETP mice

Differentially expressed hepatic genes in HFD-fed APOE3L.CETP mice		
Symbol	**Name**	**Fold Change (HFD vs LFD)**
Orm3	orosomucoid 3	**7.76**
Cyp7a1	Cholesterol 7 alpha-hydroxylase (or cytochrome P450 7A1)	**2.55**
Pparg	peroxisome proliferator activated receptor gamma	**2.47**
Saa1	serum amyloid A 1	**1.88**
Saa3	serum amyloid A 3	**1.72**
Pcsk9	proprotein convertase subtilisin/kexin type 9	**-1.89**
Fasn	fatty acid synthase	**-1.89**
Sik1	salt inducible kinase 1	**-1.92**
Lepr	leptin receptor	**-3.33**
Sqle	squalene epoxidase	**-4.87**

We validated that the expression of *Orm3*, *Cyp7a1*, *Pparg*, *Saa1* and *Saa3* in 12-weeks HFD-fed APOE3L.CETP was up-regulated while the expression of *Pcsk9*, *Fasn*, *Sik1*, *Lepr* and *Sqle* was indeed downregulated.

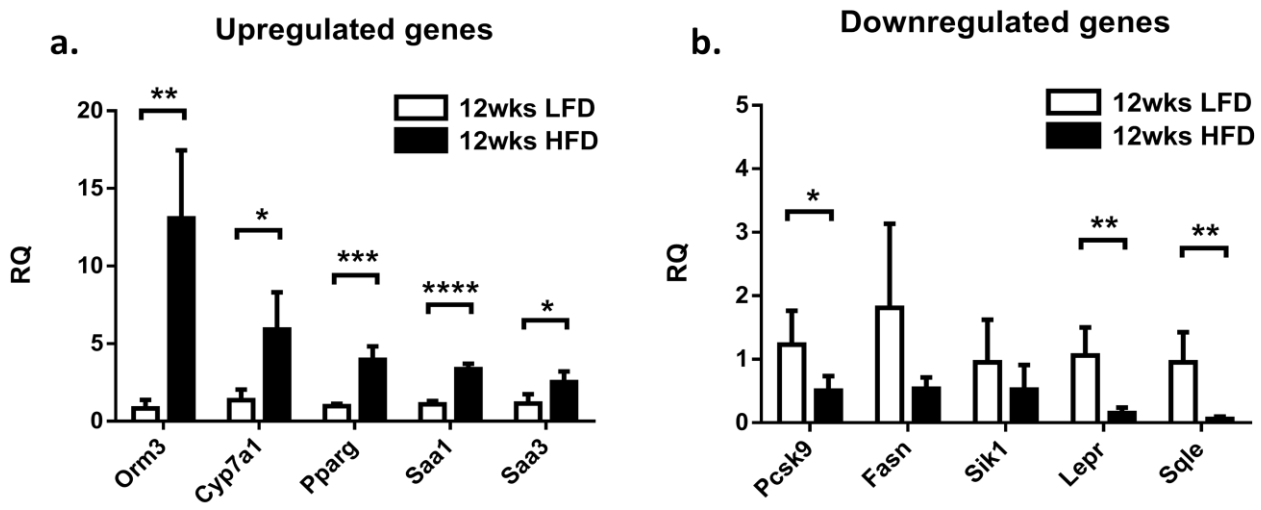

Figure 19: Expression analysis of differentially expressed genes livers in 12-weeks HFD fed (N=4) versus 12-weeks LFD fed APOE3L.CETP mice. Data is shown as RQ. All values represent the mean ± S.D. Student's t-test was performed. **P*<0.05, ***P*<0.01, ****P*<0.001, *****P*<0.0001.

Pparg is a master transcription factor of adipose tissue development, which can induce the whole program of adipogenesis (Chawla et al., 1994; Rosen et al., 1999; Siersbaek et al., 2010). The fact that its expression levels are elevated in mice with metabolic syndrome can be interpreted by the observed fat tissue overgrowth which renders these mice obese.

Orm3, a member of Alpha-1-acid glycoprotein (AGP) family, is considered to be an acute phase response protein whose levels increase under certain conditions such as systemic tissue injury and inflammation (Fournier et al., 2000). For this reason, we could reasonably attribute its increased expression in livers of 12-weeks HFD-fed mice to the low grade inflammation state that characterizes Metabolic Syndrome. Furthermore, this protein family seems to play a crucial role in sphingolipid metabolism mainly by acting as negative regulators of their synthesis (Breslow et al., 2010). So, by being involved in metabolism regulation is has been also proposed as a promising factor related to obesity, metabolic syndrome and cardiovascular diseases (Luo et al., 2015).

Saa1 and *Saa3* belong to the serum amyloid α family, are mainly produced in the liver and their expression is induced in response to inflammatory stimuli (Uhlar and Whitehead, 1999). Thus their overexpression in livers of mice with metabolic syndrome seems to represent a response mechanism due to the systemic inflammation.

Cyp7a1 belongs to the family of cytochrome P450 that play crucial roles in cholesterol metabolism and mediates the catabolism of cholesterol to bile acids in the liver (Lorbek et al., 2012). Gain-of-function experiments in mice have already shown that overexpression of *Cyp7a1* results in lowering of LDL plasma levels (Spady et al., 1998) so the increased levels in our mice could imply a response mechanism to hyperlipidemia.

Pcsk9 encodes for an enzyme that can bind to the LDL receptor (LDLR) and inhibit its function in removing the LDL particles from the circulation (Norata et al., 2016). As a consequence, in the liver *Pcsk9* promotes the degradation of hepatic LDLR receptor and thereby increases blood cholesterol, triglycerides and apoB containing particles (Rashid et al., 2014). For these reasons *Pcsk9* has been correlated with the development of atherosclerosis and hepatic lipogenesis (Tavori et al., 2016), while its inhibition seems to be promising therapeutic approach for alleviating these disorders.

On the other hand, *Fasn* is a lipogenic gene that encodes for the fatty acid synthase enzyme which catalyzes the de novo synthesis of fatty acid (Jensen-Urstad and Semenkovich, 2012). In our experiments, we observe that *Pcsk9* and *Fasn* are significantly downregulated in 12-weeks HFD mice and we could again hypothesize the presence of a self-defense mechanism to hyperlipidemia.

Lepr gene encodes for leptin receptor which is crucial for the leptin signaling pathway which controls adipose tissue mass. Deficiency and mutations in *Lepr* are associated with early-onset of obesity in mice (Clement et al., 1998) and these observations are in agreement with our results that indicate a clear downregulation of this gene in metabolic syndrome.

Sqle encodes for squalene epoxidase which catalyzes the first oxygenation step in sterol biosynthesis. Research in HepG2 cells has shown that the activity of this enzyme is decreased upon LDL treatments (Hidaka et al., 1990). This resembles the state of mice with metabolic syndrome which present high LDL cholesterol levels and we could hypothesize that squalene epoxidase is regulated at the transcription level.

Lastly, *Sik1* plays regulatory roles during steroidogenesis, lipogenesis and gluconeogenesis (Katoh et al., 2004; Patel et al., 2014) and its downregulation in 12-

weeks HFD-fed APOE3L.CETP mice could possibly contribute to the development of Metabolic Syndrome and its comorbidities as we will discuss later on.

iv) Searching for predicted targets of the up-regulated microRNAs in the differentially expressed genes of liver microarrays of APOE3L.CETP mice

Next, we pursued to take advantage of the transcriptomic analysis in the livers of 12 weeks HFD-fed APOE3L.CETP mice in order to unravel potential miRNA target genes. For this reason, we used the online computational prediction tools miRDB (Wang, 2010) and TargetScan (Agarwal et al., 2015) to identify predicted targets of miR-27a, miR-130b and miR-193b that were found to be increased in the circulation of 12-weeks HFD-fed APOE3L.CETP mice. By searching the top differentially expressed genes in the liver microarray data and combining our prediction findings we ended up with the following table:

Table 19: Several predicted target genes of the upregulated microRNAs were found to be differentially expressed in liver microarrays.

microRNA	Symbol	Gene Name	Fold Change HFD vs LFD	Biological process
miR-27a	**Pparg**	peroxisome proliferator activated receptor gamma	**2,47**	Regulation of lipid metabolic process
	Cyp39a1	cytochrome P450, family 39, subfamily a, polypeptide 1	**-1.9**	Lipid metabolic process
	Sik1	salt inducible kinase 1	**-1.92**	Regulation of triglyceride biosynthesis and gluconeogenesis
miR-130b	**Pparg**	peroxisome proliferator activated receptor gamma	**2,47**	Regulation of lipid metabolic process
	Atp2b2	ATPase, Ca++ transporting, plasma membrane 2	**-1.83**	ATP catabolic process, calcium ion transport
	Btg1	B cell translocation gene 1	**-1.63**	Regulation of angiogenesis
	Sik1	salt inducible kinase 1	**-1.92**	Regulation of triglyceride biosynthesis and gluconeogenesis
miR-193b	**Adam11**	a disintegrin and metallopeptidase domain 11	**1.92**	Integrin-mediated signalling pathway

Salt inducible kinase 1 (Sik1) which was downregulated in the liver microarrays was found to be a predicted target of both miR-27a and miR-130b that were found upregulated in the serum. Since Sik1 is involved in metabolic biological processes such as triglyceride biosynthesis and gluconeogenesis we attempted to unravel a possible interaction in order to identify a potential regulatory mechanism in the pathogenesis of Metabolic Syndrome.

Initially, by using the miRDB online tool we found that miR-27a presents a higher score in targeting Sik1 3'UTR so we decided to focus on miR-27a. By searching in miRDB online tool we detected the binding sequence of miR-27a and its predicted target site on Sik1 3'UTR (Figure 20).

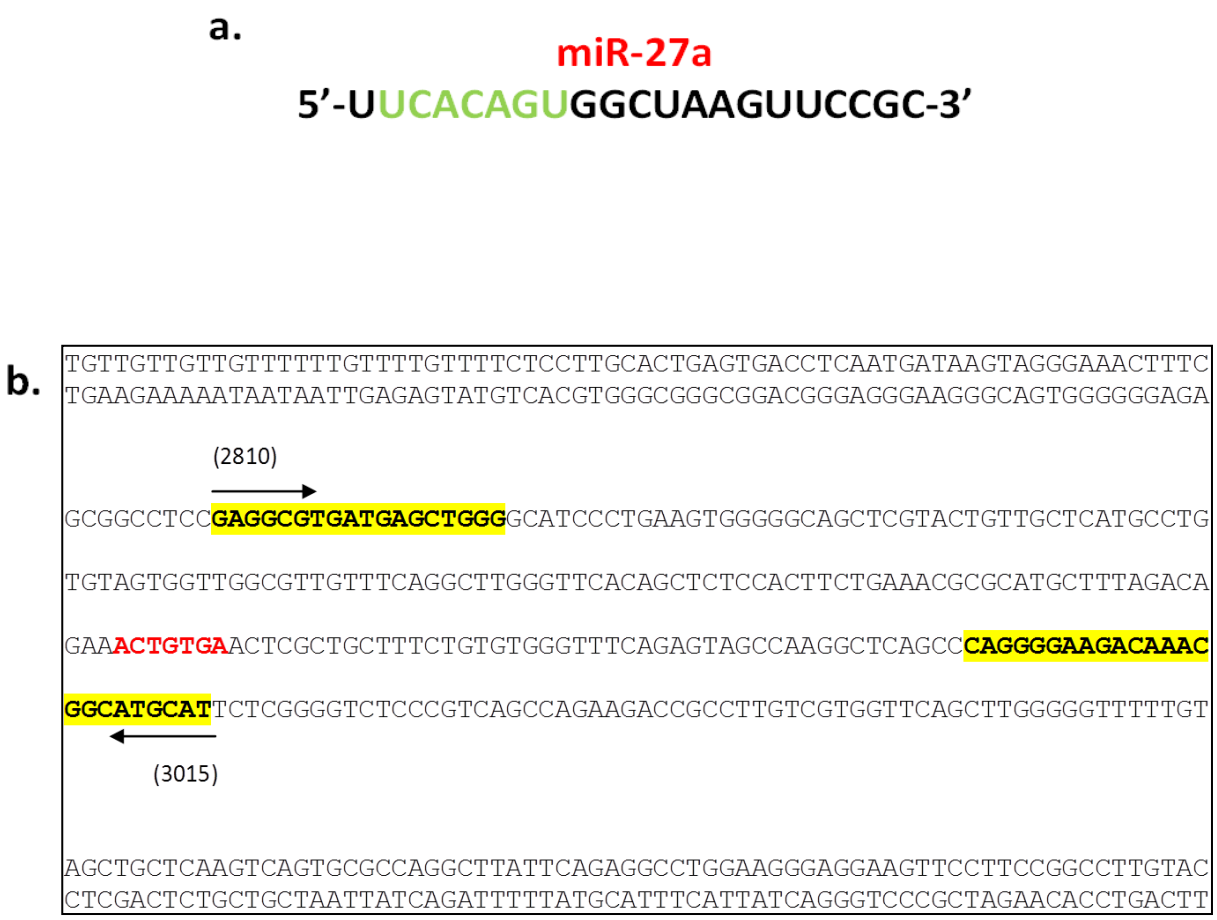

Figure 20: **a.** miR-27a and its binding sequence to Sik1 3'UTR, **b.** the target sequence of miR-27a in the Sik1 3'UTR (red letters), the selected primers (yellow shade) and their sites.

Since the 3' UTR of Salt Inducible Kinase 1 contains a predicted target site for miR-27a we decided to set up a luciferase reporter assay in HEPA (mouse hepatoma) cells. For this reason we wanted to amplify a sequence of Sik1-3'UTR (206bp) that contains the predicted target site for miR-27a (Figure 20) by using specific primers (Table 10) in order to insert it in pGL3 promoter vector downstream of the luciferase gene (Figure 23).

Firstly, we amplified the requested sequence in a small scale PCR (Figure 21a) and subsequently we performed three additional large-scale PCR reactions in order to obtain our sequence in more copies (Figure 21b).

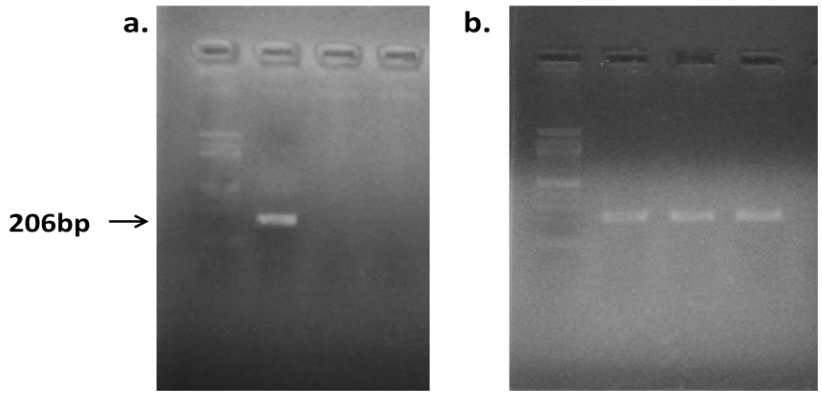

Figure 21. Sik1-3'UTR PCR product (206bp) a) in a small scale-test reaction (25μL), b) in 3 large scale reactions (50μL).

Moreover, to verify that our pGL3 promoter was the correct vector, we performed two digestions with the restriction enzymes XbaI and HindIII / KpnI which give one linear fragment of 5010bp and two fragments of 4770bp and 240pb respectively, according to the vector map (Figure 14). Indeed we identified these specific fragments and we validated that pGL3 promoter plasmid is correct (Figure 22).

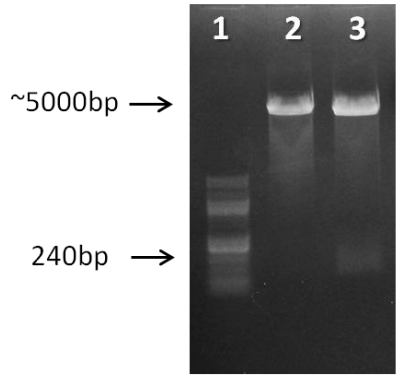

Figure 22. pGL3 promoter vector digested with 2) XbaI and 3) HindIII/KpnI. 1) 100bp DNA ladder, NEB.

Consequently, we proceeded to a ligation reaction between Sik1-3'UTR insert and pGL3 promoter vector both restricted with XbaI and we transformed DH10β competent bacteria cells with our constructs.

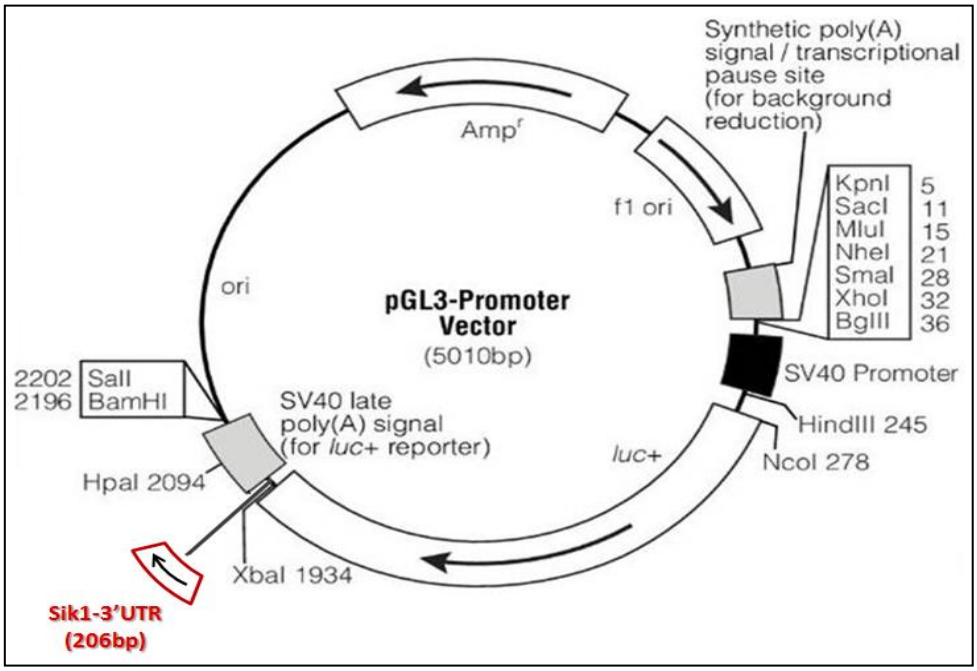

Figure 23. The site and the orientation of Sik1-3'UTR insert sequence in pGL3 promoter vector. Ligation was performed in the XbaI (1934) site of the vector by digesting both the vector and the insert with XbaI.

Afterwards, minipreps were performed in a number of bacterial colonies and plasmid DNAs were restricted with BamHI in order to validate that our product was correct and that the orientation of our insert was the appropriate. If the orientation is correct (Figure 23) BamHI digestion will give two fragments of 468bp and 4748bp as the constructs will have two BamHI sites (the first from the vector and the second will have been introduced by the FW primer, Table 10). As we observe in the vector map, the pGL3-promoter vector gives two bands of 262bp and 4748bp upon double digestion with XbaI and BamHI, which was indeed validated in our digestion experiments (Figure 24, No16). Here, we managed to identify one positive bacterial colony, in which BamHI digestion gave one band of 468bp, apart from the vector backbone (4748bp), which indicates that the vector had incorporated our insert with the desired orientation (Figure 24, No15).

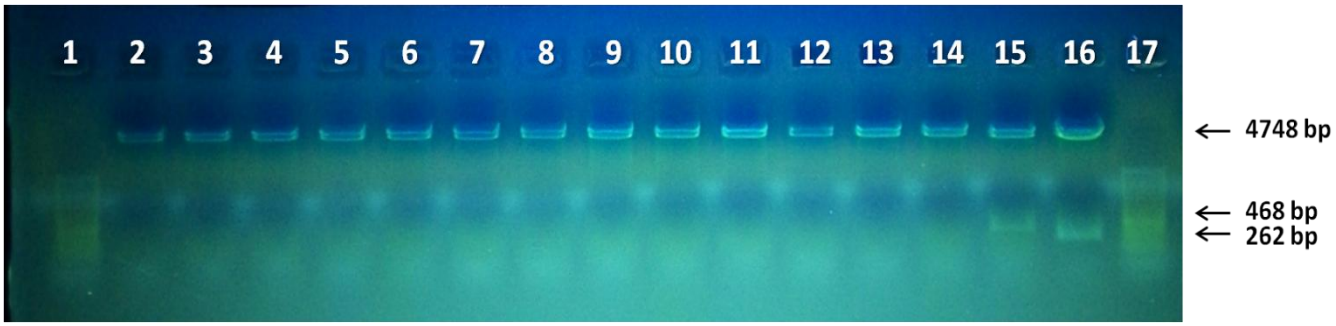

Figure 24. Digestions of plasmid DNAs and the empty pGL3-promoter vector. (1, 17): ladder (λ DNA-BstEII Digest, NEB), (2-15): plasmid DNAs from unique bacterial colonies digested with BamHI, (16): empty pGL3-promoter vector digested with BamHI/XbaI.

Lastly, we are planning to transfect HEPA cells with our construct and perform simultaneous treatments with mimic and anti-miR-27a. If miR-27a targets Sik1-3'UTR and our hypothesis is correct we should expect a decrease in luciferase reporter activity.

CONCLUSIONS – FUTURE DIRECTIONS

Our findings indicate the presence of specific signatures in liver gene expression and serum miRNA levels in 12-week HFD-fed APOE3L.CETP mice which suffer from Metabolic Syndrome. We saw that circulating miR-27a, miR-130b and miR-193b levels were elevated so they could be possibly used as biomarkers of the disease. Furthermore, we showed that none of these miRNAs were upregulated in the serum of diabetic mice, meaning that their increase in the serum of APOE3L.CETP mice could not be attributed to diabetic parameters of MetS. On the other hand, circulating miR-192, miR-194 and miR-223 were found to be elevated in the circulation of diabetic Akt2-/- mice so further experiments are needed to be done in humans in order to be exploited as putative biomarkers of T2DM.

Furthermore, our experiments validated the findings of liver microarrays in the 12-week HFD group which unraveled novel genes that are differentially expressed during the course of Metabolic Syndrome development. Functional experiments must be done in vitro and in vivo in order to verify whether these genes play a causative role in the developments and/or the progression of the disease.

Lastly, one finding that intrigued us was the downregulation of Sik1 in the livers of 12-weeks HFD-fed APOE3L.CETP mice and its potential regulation by miR-27a. As we have already mentioned above, a recent study showed that Sik1 can activate SR-BI receptor in adrenals through direct phosphorylation and as a result it enhances the selective transport of cholesteryl esters (CE) from HDL into the adrenals. However, this regulatory mechanism has not been found to exist in the liver, so possibly this kinase could also exert a crucial role in regulating HDL-CE uptake from the circulation to the liver and their subsequent degradation to bile acids. So interestingly, the downregulation of Sik1 could imply a decreased activation of SR-BI receptor and therefore a disturbed HDL-CE uptake by the liver. SR-BI expression levels in liver were found to be unaffected in 12 weeks of HFD feeding (data not shown) enhancing the possibility of a post-translational regulation of the receptor by phosphorylation. If this hypothesis is correct, CE could possibly remain bound on HDL attenuating its capacity for loading new CE molecules from other tissues (e.g. macrophages) and thus blocking

the removal of excess cholesterol from the periphery. Remarkably, SR-BI Tg mice, that overexpress SR-BI, present an accelerated clearance of HDL, revealing the importance of this receptor in HDL physiology (Ji et al., 1999). We have observed that 12-week HFD-fed APOE3L.CETP mice exert increased total plasma cholesterol and HDL levels (data not shown) which are consistent with the observations in SR-BI$^{-/-}$ mice (Rigotti et al., 1997). Collectively, the non effective removal of excess cholesterol from the periphery by HDL could be a factor that promotes the development of atherosclerosis in HFD-fed mice and SR-BI might play a pivotal role.

Thus it could be plausible to investigate the role of Sik1 in the regulation of HDL clearance through SR-BI in the liver and if the disturbance of this process could lead to the already characterized atherosclerotic phenotype of APOE3L.CETP mice (Westerterp et al., 2006; Zadelaar et al., 2007). Furthermore, if Sik1 is proved to be a direct target of miR-27a and since its levels are increased in the circulation of HFD-fed APOE3L.CETP mice, inhibition of this miR could serve a potential therapeutic approach to alleviate the atherosclerotic aspect of Metabolic Syndrome.

REFERENCES

Agarwal, P., R. Srivastava, A.K. Srivastava, S. Ali, and M. Datta. 2013. miR-135a targets IRS2 and regulates insulin signaling and glucose uptake in the diabetic gastrocnemius skeletal muscle. *Biochimica et biophysica acta*. 1832:1294-1303.

Agarwal, V., G.W. Bell, J.W. Nam, and D.P. Bartel. 2015. Predicting effective microRNA target sites in mammalian mRNAs. *eLife*. 4.

Alberti, K.G., R.H. Eckel, S.M. Grundy, P.Z. Zimmet, J.I. Cleeman, K.A. Donato, J.C. Fruchart, W.P. James, C.M. Loria, and S.C. Smith, Jr. 2009. Harmonizing the metabolic syndrome: a joint interim statement of the International Diabetes Federation Task Force on Epidemiology and Prevention; National Heart, Lung, and Blood Institute; American Heart Association; World Heart Federation; International Atherosclerosis Society; and International Association for the Study of Obesity. *Circulation*. 120:1640-1645.

Alberti, K.G., P. Zimmet, and J. Shaw. 2005. The metabolic syndrome--a new worldwide definition. *Lancet (London, England)*. 366:1059-1062.

Arroyo, J.D., J.R. Chevillet, E.M. Kroh, I.K. Ruf, C.C. Pritchard, D.F. Gibson, P.S. Mitchell, C.F. Bennett, E.L. Pogosova-Agadjanyan, D.L. Stirewalt, J.F. Tait, and M. Tewari. 2011. Argonaute2 complexes carry a population of circulating microRNAs independent of vesicles in human plasma. *Proceedings of the National Academy of Sciences of the United States of America*. 108:5003-5008.

Barzilay, J.I., L. Abraham, S.R. Heckbert, M. Cushman, L.H. Kuller, H.E. Resnick, and R.P. Tracy. 2001. The relation of markers of inflammation to the development of glucose disorders in the elderly: the Cardiovascular Health Study. *Diabetes*. 50:2384-2389.

Becker, P.P., M. Rau, J. Schmitt, C. Malsch, C. Hammer, H. Bantel, B. Mullhaupt, and A. Geier. 2015. Performance of Serum microRNAs -122, -192 and -21 as Biomarkers in Patients with Non-Alcoholic Steatohepatitis. *PloS one*. 10:e0142661.

Belarbi, Y., N. Mejhert, S. Lorente-Cebrian, I. Dahlman, P. Arner, M. Ryden, and A. Kulyte. 2015. MicroRNA-193b Controls Adiponectin Production in Human White Adipose Tissue. *The Journal of clinical endocrinology and metabolism*. 100:E1084-1088.

BERDEAUX, R. 2011. Metabolic regulation by salt inducible kinases. *Front. Biol.* 6:231-241.

Besler, C., T.F. Luscher, and U. Landmesser. 2012. Molecular mechanisms of vascular effects of High-density lipoprotein: alterations in cardiovascular disease. *EMBO molecular medicine*. 4:251-268.

Breslow, D.K., S.R. Collins, B. Bodenmiller, R. Aebersold, K. Simons, A. Shevchenko, C.S. Ejsing, and J.S. Weissman. 2010. Orm family proteins mediate sphingolipid homeostasis. *Nature*. 463:1048-1053.

Chawla, A., E.J. Schwarz, D.D. Dimaculangan, and M.A. Lazar. 1994. Peroxisome proliferator-activated receptor (PPAR) gamma: adipose-predominant expression and induction early in adipocyte differentiation. *Endocrinology*. 135:798-800.

Chen, C., Y. Peng, Y. Peng, J. Peng, and S. Jiang. 2014. miR-135a-5p inhibits 3T3-L1 adipogenesis through activation of canonical Wnt/beta-catenin signaling. *Journal of molecular endocrinology*. 52:311-320.

Chen, Z., J. Luo, L. Ma, H. Wang, W. Cao, H. Xu, J. Zhu, Y. Sun, J. Li, D. Yao, K. Kang, and D. Gou. 2015. MiR130b-Regulation of PPARgamma Coactivator- 1alpha Suppresses Fat Metabolism in Goat Mammary Epithelial Cells. *PloS one*. 10:e0142809.

Chi, H. 2015. miR-194 regulated AGK and inhibited cell proliferation of oral squamous cell carcinoma by reducing PI3K-Akt-FoxO3a signaling. *Biomedicine & pharmacotherapy = Biomedecine & pharmacotherapie*. 71:53-57.

Cho, H., J. Mu, J.K. Kim, J.L. Thorvaldsen, Q. Chu, E.B. Crenshaw, 3rd, K.H. Kaestner, M.S. Bartolomei, G.I. Shulman, and M.J. Birnbaum. 2001. Insulin resistance and a diabetes mellitus-like syndrome in mice lacking the protein kinase Akt2 (PKB beta). *Science*. 292:1728-1731.

Clement, K., C. Vaisse, N. Lahlou, S. Cabrol, V. Pelloux, D. Cassuto, M. Gourmelen, C. Dina, J. Chambaz, J.M. Lacorte, A. Basdevant, P. Bougneres, Y. Lebouc, P. Froguel, and B. Guy-Grand. 1998. A mutation in the human leptin receptor gene causes obesity and pituitary dysfunction. *Nature*. 392:398-401.

DeFronzo, R.A. 1992. Pathogenesis of type 2 (non-insulin dependent) diabetes mellitus: a balanced overview. *Diabetologia*. 35:389-397.

DeFronzo, R.A., and D. Tripathy. 2009. Skeletal muscle insulin resistance is the primary defect in type 2 diabetes. *Diabetes care*. 32 Suppl 2:S157-163.

Esau, C., S. Davis, S.F. Murray, X.X. Yu, S.K. Pandey, M. Pear, L. Watts, S.L. Booten, M. Graham, R. McKay, A. Subramaniam, S. Propp, B.A. Lollo, S. Freier, C.F. Bennett, S. Bhanot, and B.P. Monia. 2006. miR-122 regulation of lipid metabolism revealed by in vivo antisense targeting. *Cell metabolism*. 3:87-98.

Festa, A., R. D'Agostino, Jr., R.P. Tracy, and S.M. Haffner. 2002. Elevated levels of acute-phase proteins and plasminogen activator inhibitor-1 predict the development of type 2 diabetes: the insulin resistance atherosclerosis study. *Diabetes*. 51:1131-1137.

Ford, E.S., W.H. Giles, and W.H. Dietz. 2002. Prevalence of the metabolic syndrome among US adults: findings from the third National Health and Nutrition Examination Survey. *Jama*. 287:356-359.

Fournier, T., N.N. Medjoubi, and D. Porquet. 2000. Alpha-1-acid glycoprotein. *Biochimica et biophysica acta*. 1482:157-171.

Garofalo, R.S., S.J. Orena, K. Rafidi, A.J. Torchia, J.L. Stock, A.L. Hildebrandt, T. Coskran, S.C. Black, D.J. Brees, J.R. Wicks, J.D. McNeish, and K.G. Coleman. 2003. Severe diabetes, age-dependent loss of adipose tissue, and mild growth deficiency in mice lacking Akt2/PKB beta. *The Journal of clinical investigation*. 112:197-208.

Genser, L., J.R. Casella Mariolo, L. Castagneto-Gissey, S. Panagiotopoulos, and F. Rubino. 2016. Obesity, Type 2 Diabetes, and the Metabolic Syndrome: Pathophysiologic Relationships

and Guidelines for Surgical Intervention. *The Surgical clinics of North America*. 96:681-701.

Guay, C., and R. Regazzi. 2013. Circulating microRNAs as novel biomarkers for diabetes mellitus. *Nature reviews. Endocrinology*. 9:513-521.

Guilherme, A., J.V. Virbasius, V. Puri, and M.P. Czech. 2008. Adipocyte dysfunctions linking obesity to insulin resistance and type 2 diabetes. *Nature reviews. Molecular cell biology*. 9:367-377.

Hajer, G.R., T.W. van Haeften, and F.L. Visseren. 2008. Adipose tissue dysfunction in obesity, diabetes, and vascular diseases. *European heart journal*. 29:2959-2971.

Heneghan, H.M., N. Miller, O.J. McAnena, T. O'Brien, and M.J. Kerin. 2011. Differential miRNA expression in omental adipose tissue and in the circulation of obese patients identifies novel metabolic biomarkers. *The Journal of clinical endocrinology and metabolism*. 96:E846-850.

Hidaka, Y., T. Satoh, and T. Kamei. 1990. Regulation of squalene epoxidase in HepG2 cells. *Journal of lipid research*. 31:2087-2094.

Higuchi, C., A. Nakatsuka, J. Eguchi, S. Teshigawara, M. Kanzaki, A. Katayama, S. Yamaguchi, N. Takahashi, K. Murakami, D. Ogawa, S. Sasaki, H. Makino, and J. Wada. 2015. Identification of circulating miR-101, miR-375 and miR-802 as biomarkers for type 2 diabetes. *Metabolism: clinical and experimental*. 64:489-497.

Hsieh, C.H., C.S. Rau, S.C. Wu, J.C. Yang, Y.C. Wu, T.H. Lu, S.L. Tzeng, C.J. Wu, and C.W. Lin. 2015. Weight-reduction through a low-fat diet causes differential expression of circulating microRNAs in obese C57BL/6 mice. *BMC genomics*. 16:699.

Hu, Z., J. Hu, W.J. Shen, F.B. Kraemer, and S. Azhar. 2015. A Novel Role of Salt-Inducible Kinase 1 (SIK1) in the Post-Translational Regulation of Scavenger Receptor Class B Type 1 Activity. *Biochemistry*. 54:6917-6930.

Jackson, R.J., and N. Standart. 2007. How do microRNAs regulate gene expression? *Science's STKE : signal transduction knowledge environment*. 2007:re1.

Jensen-Urstad, A.P., and C.F. Semenkovich. 2012. Fatty acid synthase and liver triglyceride metabolism: housekeeper or messenger? *Biochimica et biophysica acta*. 1821:747-753.

Ji, Y., N. Wang, R. Ramakrishnan, E. Sehayek, D. Huszar, J.L. Breslow, and A.R. Tall. 1999. Hepatic scavenger receptor BI promotes rapid clearance of high density lipoprotein free cholesterol and its transport into bile. *The Journal of biological chemistry*. 274:33398-33402.

Jia, Y., M. Guan, Z. Zheng, Q. Zhang, C. Tang, W. Xu, Z. Xiao, L. Wang, and Y. Xue. 2016. miRNAs in Urine Extracellular Vesicles as Predictors of Early-Stage Diabetic Nephropathy. *Journal of diabetes research*. 2016:7932765.

Jiang, Z.Y., Q.L. Zhou, K.A. Coleman, M. Chouinard, Q. Boese, and M.P. Czech. 2003. Insulin signaling through Akt/protein kinase B analyzed by small interfering RNA-mediated gene silencing. *Proceedings of the National Academy of Sciences of the United States of America*. 100:7569-7574.

Kakafika, A., V.G. Athyros, K. Tziomalos, A. Karagiannis, and D.P. Mikhailidis. 2008. High density lipoprotein cholesterol and statin trials. *Current medicinal chemistry*. 15:2265-2270.

Kardassis, D., I. Mosialou, M. Kanaki, I. Tiniakou, and E. Thymiakou. 2014. Metabolism of HDL and its regulation. *Current medicinal chemistry*. 21:2864-2880.

Karolina, D.S., S. Tavintharan, A. Armugam, S. Sepramaniam, S.L. Pek, M.T. Wong, S.C. Lim, C.F. Sum, and K. Jeyaseelan. 2012. Circulating miRNA profiles in patients with metabolic syndrome. *The Journal of clinical endocrinology and metabolism*. 97:E2271-2276.

Katoh, Y., H. Takemori, N. Horike, J. Doi, M. Muraoka, L. Min, and M. Okamoto. 2004. Salt-inducible kinase (SIK) isoforms: their involvement in steroidogenesis and adipogenesis. *Molecular and cellular endocrinology*. 217:109-112.

Katome, T., T. Obata, R. Matsushima, N. Masuyama, L.C. Cantley, Y. Gotoh, K. Kishi, H. Shiota, and Y. Ebina. 2003. Use of RNA interference-mediated gene silencing and adenoviral overexpression to elucidate the roles of AKT/protein kinase B isoforms in insulin actions. *The Journal of biological chemistry*. 278:28312-28323.

Kaur, J. 2014. A comprehensive review on metabolic syndrome. *Cardiology research and practice*. 2014:943162.

Kim, S.Y., A.Y. Kim, H.W. Lee, Y.H. Son, G.Y. Lee, J.W. Lee, Y.S. Lee, and J.B. Kim. 2010. miR-27a is a negative regulator of adipocyte differentiation via suppressing PPARgamma expression. *Biochemical and biophysical research communications*. 392:323-328.

Kohn, A.D., S.A. Summers, M.J. Birnbaum, and R.A. Roth. 1996. Expression of a constitutively active Akt Ser/Thr kinase in 3T3-L1 adipocytes stimulates glucose uptake and glucose transporter 4 translocation. *The Journal of biological chemistry*. 271:31372-31378.

Krutzfeldt, J., N. Rosch, J. Hausser, M. Manoharan, M. Zavolan, and M. Stoffel. 2012. MicroRNA-194 is a target of transcription factor 1 (Tcf1, HNF1alpha) in adult liver and controls expression of frizzled-6. *Hepatology (Baltimore, Md.)*. 55:98-107.

Latouche, C., A. Natoli, M. Reddy-Luthmoodoo, S.E. Heywood, J.A. Armitage, and B.A. Kingwell. 2016. MicroRNA-194 Modulates Glucose Metabolism and Its Skeletal Muscle Expression Is Reduced in Diabetes. *PloS one*. 11:e0155108.

Lee, R.C., R.L. Feinbaum, and V. Ambros. 1993. The C. elegans heterochronic gene lin-4 encodes small RNAs with antisense complementarity to lin-14. *Cell*. 75:843-854.

Leon, B.M., and T.M. Maddox. 2015. Diabetes and cardiovascular disease: Epidemiology, biological mechanisms, treatment recommendations and future research. *World journal of diabetes*. 6:1246-1258.

Liao, J., A. Barthel, K. Nakatani, and R.A. Roth. 1998. Activation of protein kinase B/Akt is sufficient to repress the glucocorticoid and cAMP induction of phosphoenolpyruvate carboxykinase gene. *The Journal of biological chemistry*. 273:27320-27324.

Lin, X.Z., J. Luo, L.P. Zhang, W. Wang, H.B. Shi, and J.J. Zhu. 2013. MiR-27a suppresses triglyceride accumulation and affects gene mRNA expression associated with fat metabolism in dairy goat mammary gland epithelial cells. *Gene*. 521:15-23.

Lin, Y., and Z. Sun. 2010. Current views on type 2 diabetes. *The Journal of endocrinology*. 204:1-11.

Lonardo, A. 1999. Fatty liver and nonalcoholic steatohepatitis. Where do we stand and where are we going? *Digestive diseases (Basel, Switzerland)*. 17:80-89.

Lorbek, G., M. Lewinska, and D. Rozman. 2012. Cytochrome P450s in the synthesis of cholesterol and bile acids--from mouse models to human diseases. *The FEBS journal*. 279:1516-1533.

Lu, H., R.J. Buchan, and S.A. Cook. 2010. MicroRNA-223 regulates Glut4 expression and cardiomyocyte glucose metabolism. *Cardiovascular research*. 86:410-420.

Luo, Z., H. Lei, Y. Sun, X. Liu, and D.F. Su. 2015. Orosomucoid, an acute response protein with multiple modulating activities. *Journal of physiology and biochemistry*. 71:329-340.

Lusis, A.J. 2000. Atherosclerosis. *Nature*. 407:233-241.

Ma, X., C. Lu, C. Lv, C. Wu, and Q. Wang. 2016. The Expression of miR-192 and Its Significance in Diabetic Nephropathy Patients with Different Urine Albumin Creatinine Ratio. *Journal of diabetes research*. 2016:6789402.

Marchesini, G., M. Brizi, G. Bianchi, S. Tomassetti, E. Bugianesi, M. Lenzi, A.J. McCullough, S. Natale, G. Forlani, and N. Melchionda. 2001. Nonalcoholic fatty liver disease: a feature of the metabolic syndrome. *Diabetes*. 50:1844-1850.

Moller, D.E., and K.D. Kaufman. 2005. Metabolic syndrome: a clinical and molecular perspective. *Annual review of medicine*. 56:45-62.

Norata, G.D., H. Tavori, A. Pirillo, S. Fazio, and A.L. Catapano. 2016. Biology of PCSK9: beyond LDL cholesterol lowering. *Cardiovascular research*.

Out, R., M. Hoekstra, J.A. Spijkers, J.K. Kruijt, M. van Eck, I.S. Bos, J. Twisk, and T.J. Van Berkel. 2004. Scavenger receptor class B type I is solely responsible for the selective uptake of cholesteryl esters from HDL by the liver and the adrenals in mice. *Journal of lipid research*. 45:2088-2095.

Parrizas, M., L. Brugnara, Y. Esteban, A. Gonzalez-Franquesa, S. Canivell, S. Murillo, E. Gordillo-Bastidas, R. Cusso, J.A. Cadefau, P.M. Garcia-Roves, J.M. Servitja, and A. Novials. 2015. Circulating miR-192 and miR-193b are markers of prediabetes and are modulated by an exercise intervention. *The Journal of clinical endocrinology and metabolism*. 100:E407-415.

Patel, K., M. Foretz, A. Marion, D.G. Campbell, R. Gourlay, N. Boudaba, E. Tournier, P. Titchenell, M. Peggie, M. Deak, M. Wan, K.H. Kaestner, O. Goransson, B. Viollet, N.S. Gray, M.J. Birnbaum, C. Sutherland, and K. Sakamoto. 2014. The LKB1-salt-inducible kinase pathway functions as a key gluconeogenic suppressor in the liver. *Nature communications*. 5:4535.

Poy, M.N., L. Eliasson, J. Krutzfeldt, S. Kuwajima, X. Ma, P.E. Macdonald, S. Pfeffer, T. Tuschl, N. Rajewsky, P. Rorsman, and M. Stoffel. 2004. A pancreatic islet-specific microRNA regulates insulin secretion. *Nature*. 432:226-230.

Rashid, S., H. Tavori, P.E. Brown, M.F. Linton, J. He, I. Giunzioni, and S. Fazio. 2014. Proprotein convertase subtilisin kexin type 9 promotes intestinal overproduction of triglyceride-rich apolipoprotein B lipoproteins through both low-density lipoprotein receptor-dependent and -independent mechanisms. *Circulation*. 130:431-441.

Rask-Madsen, C., and C.R. Kahn. 2012. Tissue-specific insulin signaling, metabolic syndrome, and cardiovascular disease. *Arteriosclerosis, thrombosis, and vascular biology*. 32:2052-2059.

Reilly, M.P., and D.J. Rader. 2003. The metabolic syndrome: more than the sum of its parts? *Circulation*. 108:1546-1551.

Rigotti, A., B.L. Trigatti, M. Penman, H. Rayburn, J. Herz, and M. Krieger. 1997. A targeted mutation in the murine gene encoding the high density lipoprotein (HDL) receptor scavenger receptor class B type I reveals its key role in HDL metabolism. *Proceedings of the National Academy of Sciences of the United States of America*. 94:12610-12615.

Rosen, E.D., P. Sarraf, A.E. Troy, G. Bradwin, K. Moore, D.S. Milstone, B.M. Spiegelman, and R.M. Mortensen. 1999. PPAR gamma is required for the differentiation of adipose tissue in vivo and in vitro. *Molecular cell*. 4:611-617.

Ross, R. 1993. The pathogenesis of atherosclerosis: a perspective for the 1990s. *Nature*. 362:801-809.

Rottiers, V., and A.M. Naar. 2012. MicroRNAs in metabolism and metabolic disorders. *Nature reviews. Molecular cell biology*. 13:239-250.

Samuel, V.T., K.F. Petersen, and G.I. Shulman. 2010. Lipid-induced insulin resistance: unravelling the mechanism. *Lancet*. 375:2267-2277.

Sandhofer, A., S. Kaser, A. Ritsch, M. Laimer, J. Engl, B. Paulweber, J.R. Patsch, and C.F. Ebenbichler. 2006. Cholesteryl ester transfer protein in metabolic syndrome. *Obesity*. 14:812-818.

Schmidt, M.I., B.B. Duncan, A.R. Sharrett, G. Lindberg, P.J. Savage, S. Offenbacher, M.I. Azambuja, R.P. Tracy, and G. Heiss. 1999. Markers of inflammation and prediction of diabetes mellitus in adults (Atherosclerosis Risk in Communities study): a cohort study. *Lancet*. 353:1649-1652.

Shirasaki, T., M. Honda, T. Shimakami, R. Horii, T. Yamashita, Y. Sakai, A. Sakai, H. Okada, R. Watanabe, S. Murakami, M. Yi, S.M. Lemon, and S. Kaneko. 2013. MicroRNA-27a regulates lipid metabolism and inhibits hepatitis C virus replication in human hepatoma cells. *Journal of virology*. 87:5270-5286.

Shulman, G.I. 2014a. Ectopic fat in insulin resistance, dyslipidemia, and cardiometabolic disease. *The New England journal of medicine*. 371:2237-2238.

Shulman, G.I. 2014b. Ectopic fat in insulin resistance, dyslipidemia, and cardiometabolic disease. *The New England journal of medicine*. 371:1131-1141.

Siersbaek, R., R. Nielsen, and S. Mandrup. 2010. PPARgamma in adipocyte differentiation and metabolism--novel insights from genome-wide studies. *FEBS letters*. 584:3242-3249.

Spady, D.K., J.A. Cuthbert, M.N. Willard, and R.S. Meidell. 1998. Overexpression of cholesterol 7alpha-hydroxylase (CYP7A) in mice lacking the low density lipoprotein (LDL) receptor gene. LDL transport and plasma LDL concentrations are reduced. *The Journal of biological chemistry*. 273:126-132.

Stumvoll, M., B.J. Goldstein, and T.W. van Haeften. 2005. Type 2 diabetes: principles of pathogenesis and therapy. *Lancet*. 365:1333-1346.

Sun, T., M. Fu, A.L. Bookout, S.A. Kliewer, and D.J. Mangelsdorf. 2009. MicroRNA let-7 regulates 3T3-L1 adipogenesis. *Molecular endocrinology (Baltimore, Md.)*. 23:925-931.

Tariq, S.M., M.S. Sidhu, P.P. Toth, and W.E. Boden. 2014. HDL hypothesis: where do we stand now? *Current atherosclerosis reports*. 16:398.

Tavori, H., I. Giunzioni, I.M. Predazzi, D. Plubell, A. Shivinsky, J. Miles, R.M. Devay, H. Liang, S. Rashid, M.F. Linton, and S. Fazio. 2016. Human PCSK9 promotes hepatic lipogenesis and atherosclerosis development via apoE- and LDLR-mediated mechanisms. *Cardiovascular research*. 110:268-278.

Ueki, K., R. Yamamoto-Honda, Y. Kaburagi, T. Yamauchi, K. Tobe, B.M. Burgering, P.J. Coffer, I. Komuro, Y. Akanuma, Y. Yazaki, and T. Kadowaki. 1998. Potential role of protein kinase B in insulin-induced glucose transport, glycogen synthesis, and protein synthesis. *The Journal of biological chemistry*. 273:5315-5322.

Uhlar, C.M., and A.S. Whitehead. 1999. Serum amyloid A, the major vertebrate acute-phase reactant. *European journal of biochemistry / FEBS*. 265:501-523.

van den Hoek, A.M., J.W. van der Hoorn, A.C. Maas, R.M. van den Hoogen, A. van Nieuwkoop, S. Droog, E.H. Offerman, E.J. Pieterman, L.M. Havekes, and H.M. Princen. 2014. APOE*3Leiden.CETP transgenic mice as model for pharmaceutical treatment of the metabolic syndrome. *Diabetes, obesity & metabolism*. 16:537-544.

Vassallo, P., S.L. Driver, and N.J. Stone. 2016. Metabolic Syndrome: An Evolving Clinical Construct. *Progress in cardiovascular diseases*.

Vaziri, N.D. 2016. HDL abnormalities in nephrotic syndrome and chronic kidney disease. *Nature reviews. Nephrology*. 12:37-47.

Vickers, K.C., S.R. Landstreet, M.G. Levin, B.M. Shoucri, C.L. Toth, R.C. Taylor, B.T. Palmisano, F. Tabet, H.L. Cui, K.A. Rye, P. Sethupathy, and A.T. Remaley. 2014. MicroRNA-223 coordinates cholesterol homeostasis. *Proceedings of the National Academy of Sciences of the United States of America*. 111:14518-14523.

Vickers, K.C., B.T. Palmisano, B.M. Shoucri, R.D. Shamburek, and A.T. Remaley. 2011. MicroRNAs are transported in plasma and delivered to recipient cells by high-density lipoproteins. *Nature cell biology*. 13:423-433.

Villard, A., L. Marchand, C. Thivolet, and S. Rome. 2015. Diagnostic Value of Cell-free Circulating MicroRNAs for Obesity and Type 2 Diabetes: A Meta-analysis. *Journal of molecular biomarkers & diagnosis*. 6.

Wang, L., X.J. Jia, H.J. Jiang, Y. Du, F. Yang, S.Y. Si, and B. Hong. 2013a. MicroRNAs 185, 96, and 223 repress selective high-density lipoprotein cholesterol uptake through posttranscriptional inhibition. *Molecular and cellular biology*. 33:1956-1964.

Wang, X. 2010. Computational prediction of microRNA targets. *Methods in molecular biology (Clifton, N.J.)*. 667:283-295.

Wang, Y.C., Y. Li, X.Y. Wang, D. Zhang, H. Zhang, Q. Wu, Y.Q. He, J.Y. Wang, L. Zhang, H. Xia, J. Yan, X. Li, and H. Ying. 2013b. Circulating miR-130b mediates metabolic crosstalk between fat and muscle in overweight/obesity. *Diabetologia*. 56:2275-2285.

Wang, Z., H. Takemori, S.K. Halder, Y. Nonaka, and M. Okamoto. 1999. Cloning of a novel kinase (SIK) of the SNF1/AMPK family from high salt diet-treated rat adrenal. *FEBS letters*. 453:135-139.

Westerterp, M., C.C. van der Hoogt, W. de Haan, E.H. Offerman, G.M. Dallinga-Thie, J.W. Jukema, L.M. Havekes, and P.C. Rensen. 2006. Cholesteryl ester transfer protein decreases high-density lipoprotein and severely aggravates atherosclerosis in APOE*3-Leiden mice. *Arteriosclerosis, thrombosis, and vascular biology*. 26:2552-2559.

Wightman, B., I. Ha, and G. Ruvkun. 1993. Posttranscriptional regulation of the heterochronic gene lin-14 by lin-4 mediates temporal pattern formation in C. elegans. *Cell*. 75:855-862.

Yki-Jarvinen, H. 1995. Role of insulin resistance in the pathogenesis of NIDDM. *Diabetologia*. 38:1378-1388.

Yoon, Y.S., W.Y. Seo, M.W. Lee, S.T. Kim, and S.H. Koo. 2009. Salt-inducible kinase regulates hepatic lipogenesis by controlling SREBP-1c phosphorylation. *The Journal of biological chemistry*. 284:10446-10452.

Zadelaar, S., R. Kleemann, L. Verschuren, J. de Vries-Van der Weij, J. van der Hoorn, H.M. Princen, and T. Kooistra. 2007. Mouse models for atherosclerosis and pharmaceutical modifiers. *Arteriosclerosis, thrombosis, and vascular biology*. 27:1706-1721.

Zampetaki, A., S. Kiechl, I. Drozdov, P. Willeit, U. Mayr, M. Prokopi, A. Mayr, S. Weger, F. Oberhollenzer, E. Bonora, A. Shah, J. Willeit, and M. Mayr. 2010. Plasma microRNA profiling reveals loss of endothelial miR-126 and other microRNAs in type 2 diabetes. *Circulation research*. 107:810-817.

Zhu, H., N. Shyh-Chang, A.V. Segre, G. Shinoda, S.P. Shah, W.S. Einhorn, A. Takeuchi, J.M. Engreitz, J.P. Hagan, M.G. Kharas, A. Urbach, J.E. Thornton, R. Triboulet, R.I. Gregory, D. Altshuler, and G.Q. Daley. 2011. The Lin28/let-7 axis regulates glucose metabolism. *Cell*. 147:81-94.

Zhuang, G., C. Meng, X. Guo, P.S. Cheruku, L. Shi, H. Xu, H. Li, G. Wang, A.R. Evans, S. Safe, C. Wu, and B. Zhou. 2012. A novel regulator of macrophage activation: miR-223 in obesity-associated adipose tissue inflammation. *Circulation*. 125:2892-2903.